Fizika Nizkikh Temperatur, 2011, v. 37, No. 8, p. 803–828

Impurity effects in quasiparticle spectrum of high-T_c superconductors

(Review Article)

Yu.G. Pogorelov

IFIMUP/Departamento de Física, Universidade do Porto, Rua do Campo Alegre 687, 4169-007 Porto, Portugal
E-mail: ypogorel@fc.up.pt

M.C. Santos

Departamento de Física, Universidade de Coimbra, R. Larga, Coimbra, 3004-535, Portugal

V.M. Loktev

Bogolubov Institute for Theoretical Physics, NAN of Ukraine, 14b Metrologichna Str., 03143 Kiev, Ukraine

Received March 18, 2011

The revision is made of Green function methods that describe the dynamics of electronic quasiparticles in disordered superconducting systems with *d*-wave symmetry of order parameter. Various types of impurity perturbations are analyzed within the simplest T-matrix approximation. The extension of the common self-consistent T-matrix approximation (SCTMA) to the so-called group expansions in clusters of interacting impurity centers is discussed and hence the validity criteria for SCTMA are established. A special attention is payed to the formation of impurity resonance states and localized states near the characteristic points of energy spectrum, corresponding to nodal points on the Fermi surface.

PACS: 74.20.Rp Pairing symmetries (other than s-wave);
74.62.Dh Effects of crystal defects, doping and substitution;
74.62.En Effects of disorder;
74.72.–h Cuprate superconductors.

Keywords: high-T_c superconductors, impurity states, group expansions in interacting impurity centers.

Contents

1. Introduction

This year 2011 is marked by the two remarkable anniversaries, the centennial of discovery of superconductivity (SC) as a fundamental phenomenon and the quarter-century of high-temperature SC (HTSC) in copper oxides. Both events, especially the first, made a huge impact on the development of many prospects in physics and on its ideology. Therefore, it does not look strange that many authors try to resume certain research in the field, first of all that related to their own works. And the authors of the present review article are not an exception. The topics they address are seen already from the index. Nevertheless, it can be hoped that, despite our main focus on the HTSC systems, some conclusions may be also relevant for the common, low-temperature SC systems where impurity effects are essential or disputable.

To begin with we recognize that the twenty five years of intensive study after the discovery of HTSC in perovskite metal-oxide materials [1,2] provided a solid experimental base on their electronic structure in normal and superconducting state, in particular on the specific type of SC order and its parameters [3]. However there still exist a lot of problems in theoretical understanding of fundamental physics behind the observable properties of high-T_c materials, and many of them are related to the effects of disorder by presence of impurities [4]. The impurity effects are known to be of less importance for quasiparticle dynamics and SC properties in the traditional metals and alloys with *s*-wave type of SC pairing [5,6], except for strong pair-breaking effect by paramagnetic impurities [7] and related localized impurity levels within the SC gap [8–10]. However, in the metal-oxide materials, seen as strongly doped semiconductors in the normal state [11] and displaying an *d*-wave SC order [12] below T_c, both magnetic and nonmagnetic impurities can act as effective pair-breakers [13] and produce quasiparticle resonances in the finite density of states (DOS) between the *d*-wave coherence peaks [14,15]. Such effects were already noted, though not properly recognized, in the early point-contact experiments [16] but were fully verified later on by the spectacular observations in scanning tunneling microscopy (STM) [17–19]. The further interest to the impurity effects in high-T_c materials is stimulated by their possible influence on fundamental physical properties as infrared quasiparticle conductivity [21,20], dynamics of magnetic vortices [22,23], low-temperature heat conduction [24,25], etc.

The theoretical methods for study of impurity effects in SC systems are widely adopted from the well developed general field of elementary excitations in disordered solids, beginning from the classical works by Lifshitz [26], Mott [27], and Anderson [28]. The most effective approach to the quasiparticle dynamics is provided by the Green function (GF) method [29–31], modified especially for SC quasiparticles by Gorkov [32]. The GF analysis of the disorder effects in superconductors with nontrivial symmetry of order parameter was first developed yet before the discovery of high-T_c materials, mostly based on the concept of self-consistent T-matrix approximation (SCTMA) [33–35] for the quasiparticle self-energy that describes modification of their dispersion law and lifetime under disorder. The following investigations of the effects of disorder on metal-oxide SC systems with nodal points on the quasi-2D Fermi surface lead to the conclusions on a great universality of their transport properties [36–38], and these conclusions could be also important for other Fermi systems with similar structure of excitation spectrum, as recently discovered graphene sheets [39,40].

Nevertheless, the existing dicrepancies between the predicted universal transport behavior and available experimental data [41,42], indicate a need in critical revision of the used theoretical approach. In particular, the fact that SCTMA is essentially a single-impurity approximation makes it possible that the omitted effects of inter-impurity correlations can in principle introduce important modifications into dynamics and kinetics of quasiparticles.

The main subject of this review is the theoretical work made by the authors during last ten years on validity of different approximations for GF's in disordered *d*-wave superconductors, for different types of impurity perturbations. The topic of our particular interest is the extension of the SCTMA approach to a more general form of the so-called group expansions (GE's) of self-energy [43], where the first SCTMA term is followed by a group series in increasing numbers of interacting impurity centers. They are alike the classical Ursell–Mayer group expansions in the theory of nonideal gases [44] where the particular terms (the group integrals) include physical interactions between the particles. In our case, these expansions include indirect (and, what is important, dependent on ε) interactions between the impurity centers, through the exchange by virtual excitations from (admittedly renormalized) band spectrum, so that each term corresponds to summation of a certain infinite series of diagrams. Actually, there are different types of GE's possible for particular regions of energy spectrum, one of them, called fully renormalized GE, is more adequate to extended (band-like) states and the other, nonrenormalized GE, to localized states [43,45]. Then the issue of SCTMA validity is defined by the convergence of fully renormalized GE, otherwise new important impurity effects *beyond* SCTMA can be obtained from the nonrenormalized GE as discussed in the following sections.

2. General formalism

Below we use the particular type of two-time GF's [30], since they are more adapted to the systems with intrinsic disorder than the Matsubara functions, commonly used in the field-theoretical approaches for uniform systems [31].

The Fourier transformed two-time (advanced) GF is defined as

$$\langle\langle a \,|\, b\rangle\rangle_\varepsilon = i\int\limits_{-\infty}^{0} \mathrm{e}^{i(\varepsilon - i0)t}\,\langle\{a(t), b(0)\}\rangle dt, \qquad (1)$$

where a and b are Heisenberg fermionic operators, $\langle\ldots\rangle$ is the quantum-statistical average with the corresponding Hamiltonian, and $\{.,.\}$ is the anticommutator. Various observable quantities at given temperature $T = (k_B\beta)^{-1}$ are obtained after these functions through the known spectral formula [30] for an average of operator product

$$\langle ba\rangle = \frac{1}{\pi}\int\limits_{-\infty}^{\infty} \frac{d\varepsilon}{\mathrm{e}^{\beta(\varepsilon-\mu)}+1}\langle\langle a \,|\, b\rangle\rangle_\varepsilon, \qquad (2)$$

including the chemical potential μ. The energy argument ε (in units where $\hbar = 1$) beside a GF will be dropped in what follows, unless necessary.

The explicit forms of two-time GF's can be found from the Heisenberg equation of motion for operators [30]:

$$i\frac{d}{dt}a(t) = \big[a(t), H\big],$$

where $[.,.]$ is the commutator. Then we have the related equation of motion for the Fourier transformed GF's as

$$\varepsilon\langle\langle a \,|\, b\rangle\rangle = \langle\{a, b\}\rangle + \langle\langle [a, H] \,|\, b\rangle\rangle. \qquad (3)$$

In particular, considering the operators of creation $a_{\mathbf{k}}^\dagger$ and annihilation $a_{\mathbf{k}}$ of free quasiparticles with quasimomentum $\mathbf{k}$ and eigen-energy $\varepsilon_{\mathbf{k}}$, obeying the Hamiltonian

$$H = \sum_{\mathbf{k}} \varepsilon_{\mathbf{k}} a_{\mathbf{k}}^\dagger a_{\mathbf{k}},$$

the diagonal GF $\langle\langle a_{\mathbf{k}} \,|\, a_{\mathbf{k}}^\dagger\rangle\rangle$ is simply found from Eq. (3) as

$$\langle\langle a_{\mathbf{k}} \,|\, a_{\mathbf{k}}^\dagger\rangle\rangle = \frac{1}{\varepsilon - \varepsilon_{\mathbf{k}}}.$$

A much more complicated case of interacting quasiparticles (but in a uniform system) has a general solution

$$\langle\langle a_{\mathbf{k}} \,|\, a_{\mathbf{k}}^\dagger\rangle\rangle = \frac{1}{\varepsilon - \varepsilon_{\mathbf{k}} - \Sigma_{\mathbf{k}}(\varepsilon)},$$

where the complex self-energy $\Sigma_{\mathbf{k}}(\varepsilon)$ is usually built using the diagrammatic series [31].

3. Green function method for *d*-wave superconductor

We start from the simplest single-band model for a *d*-wave superconductor (in absence of impurities), formed by 2D hopping of holes between nearest neighbor oxygen sites in CuO_2 planes [46–48] (Fig. 1). Taking explicit account of spin indices $\sigma = \uparrow, \downarrow$ and of the mean-field anomalous coupling, the Hamiltonian can be presented in the compact matrix form with use of *Nambu spinor*s, the row-spinor $\psi_{\mathbf{k}}^\dagger = (a_{\mathbf{k},\uparrow}^\dagger, a_{-\mathbf{k},\downarrow})$ and respective column-spinor $\psi_{\mathbf{k}}$:

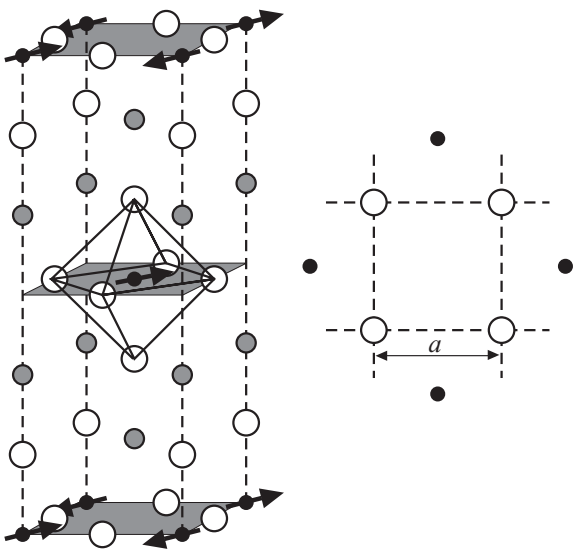

Fig. 1. The exemplary metal-oxide perovskite structure of La_2CuO_4 with conducting CuO_2 planes (shadowed) and a fragment of square lattice in such a plane. Arrows indicate AFM spin order at Cu sites.

$$H = \sum_{\mathbf{k}}\Big[\psi_{\mathbf{k}}^\dagger(\xi_{\mathbf{k}}\hat{\tau}_3 + \Delta_{\mathbf{k}}\hat{\tau}_1)\psi_{\mathbf{k}}\Big]. \qquad (4)$$

Here $\xi_{\mathbf{k}} = \varepsilon_{\mathbf{k}} - \mu$ is the energy of normal quasiparticle with quasimomentum $\mathbf{k}$ referred to the chemical potential μ (this will be also the reference for the energy variable ε) and $\hat{\tau}_j$ $(j = 1,2,3)$ are the Pauli matrices in Nambu indices. The SC pairing parameter $\Delta_{\mathbf{k}}$ satisfies the BCS gap equation [6]:

$$\Delta_{\mathbf{k}} = \frac{1}{N}\sum_{\mathbf{k}'} V_{\mathbf{k},\mathbf{k}'}\frac{\Delta_{\mathbf{k}'}}{E_{\mathbf{k}'}}\tanh\left(\frac{\beta E_{\mathbf{k}'}}{2}\right), \qquad (5)$$

where $E_{\mathbf{k}} = \sqrt{\xi_{\mathbf{k}}^2 + \Delta_{\mathbf{k}}^2}$ is the SC quasiparticle energy and the Cooper separable ansatz is used for the SC coupling function $V_{\mathbf{k},\mathbf{k}'} = V_{SC}\gamma_{\mathbf{k}}\gamma_{\mathbf{k}'}$ with the SC coupling constant V_{SC}. The coupling function $\gamma_{\mathbf{k}} = \theta(\varepsilon_D^2 - \xi_{\mathbf{k}}^2)\cos 2\varphi_{\mathbf{k}}$ includes the restriction to the BCS shell of width ε_D (the "Debye energy") around the Fermi level and the *d*-wave symmetry cosine factor with the angular variable $\varphi_{\mathbf{k}} = \arctan k_y / k_x$ for the 2D Brillouin zone. Then Eq. (5) yields in the gap function $\Delta_{\mathbf{k}} = \Delta\cos 2\varphi_{\mathbf{k}}$ where the parameter Δ is found from the specific *d*-wave gap equation:

$$1 = \frac{V_{SC}}{N}\sum_{\mathbf{k}}\frac{\theta(\varepsilon_D^2 - \xi_{\mathbf{k}}^2)\cos^2 2\varphi_{\mathbf{k}}}{\sqrt{\xi_{\mathbf{k}}^2 + \Delta^2\cos^2 2\varphi_{\mathbf{k}}}}\times$$

$$\times\tanh\left(\beta\frac{\sqrt{\xi_{\mathbf{k}}^2 + \Delta^2\cos^2 2\varphi_{\mathbf{k}}}}{2}\right). \qquad (6)$$

Next we define the 2×2 Nambu matrix of GF's:

$$\widehat{G}_{\mathbf{k},\mathbf{k}'} = \langle\langle \psi_{\mathbf{k}} \mid \psi^{\dagger}_{\mathbf{k}'} \rangle\rangle, \tag{7}$$

whose matrix elements are the well-known Gor'kov normal and anomalous functions [32]. In what follows we distinguish between the Nambu indices (N-indices) and the quasi-momentum indices (m-indices) in this matrix and in the related (more complicated) matrices. Then the exact GF matrix for the uniform system results from Eqs. (3), (4), (7) in the m-diagonal form: $\widehat{G}_{\mathbf{k},\mathbf{k}'} = \delta_{\mathbf{k},\mathbf{k}'}\widehat{G}^0_{\mathbf{k}}$, with

$$\widehat{G}^0_{\mathbf{k}} = \frac{\varepsilon + \xi_{\mathbf{k}}\hat{\tau}_3 + \Delta_{\mathbf{k}}\hat{\tau}_1}{\varepsilon^2 - E^2_{\mathbf{k}}}. \tag{8}$$

In general, the physical characteristics of SC state are suitably defined by the GF's. For instance, the electronic specific heat follows from the global single-particle DOS:

$$\rho(\varepsilon) = \pi^{-1}\mathrm{Im}\mathrm{Tr}\widehat{G}, \tag{9}$$

where $\widehat{G} = N^{-1}\sum_{\mathbf{k}}\widehat{G}_{\mathbf{k}}$ is the local GF matrix with $\widehat{G}_{\mathbf{k}} \equiv \widehat{G}_{\mathbf{k},\mathbf{k}}$. Next, the topography STM data [18] are described using the local DOS (LDOS) at **n**th lattice site:

$$\rho_{\mathbf{n}}(\varepsilon) = \frac{1}{\pi N}\sum_{\mathbf{k},\mathbf{k}'} e^{i(\mathbf{k}-\mathbf{k}')\cdot\mathbf{n}}\mathrm{Im}\mathrm{Tr}\widehat{G}_{\mathbf{k},\mathbf{k}'}. \tag{10}$$

Other observable characteristics are also expressed through GF's using the spectral formula, Eq. (2), as will be discussed in what follows.

For the 2D lattice sums, like Eqs. (6), (10) at given *d*-wave symmetry, it is suitable to use the "polar coordinates" $\xi \equiv \xi_{\mathbf{k}}$ and $\varphi \equiv \varphi_{\mathbf{k}}$, accordingly to the integration rule:

$$\frac{1}{N}\sum_{\mathbf{k}} f_{\mathbf{k}} = \left(\frac{a}{2\pi}\right)^2 \int d\mathbf{k}\, f(k_x, k_y) \approx$$

$$\approx \frac{\rho_N}{4\pi}\int\limits_{-\mu}^{W-\mu} d\xi \int\limits_{0}^{2\pi} d\varphi\, f(\xi,\varphi). \tag{11}$$

Here a is the square lattice constant and $\rho_N \approx 4/(\pi W)$ is the normal state DOS. The limits for "radial" integration (involving the bandwidth W) are rather qualitative, however they only define some less sensitive logarithmic factors.

Thus the local GF matrix for a uniform system

$$\widehat{G}^0 = \frac{1}{N}\sum_{\mathbf{k}}\widehat{G}^0_{\mathbf{k}} = \rho_N(g_0 - g_{\mathrm{as}}\hat{\tau}_3) \tag{12}$$

contains the energy dependence mainly in the function

$$g_0(\varepsilon) = \frac{\varepsilon}{N}\sum_{\mathbf{k}}\frac{1}{\varepsilon^2 - E^2_{\mathbf{k}}},$$

and from Eq. (11) (within accuracy to $O(\Delta^3/\mu^3)$) the latter is

$$g_0(\varepsilon) \approx -\mathrm{Im}\mathrm{K}\left(\frac{\Delta^2}{\varepsilon^2}\right)\mathrm{sign}\,(\varepsilon) + i\mathrm{Re}\mathrm{K}\left(\frac{\Delta^2}{\varepsilon^2}\right) + \frac{\varepsilon}{4\pi\tilde{\mu}}. \tag{13}$$

Here $\tilde{\mu} = \mu(1-\mu/W) \approx \mu$ and the complete elliptic integral of 1st kind $\mathrm{K}(k)$ behaves as [49]

$$\mathrm{K}(k) \approx \begin{cases} \pi(1+k/4)/2 & \text{at} \quad k \ll 1, \\ \ln(4/\sqrt{k-1}) & \text{at} \quad |k-1| \ll 1, \\ -i\ln(4i\sqrt{k})/\sqrt{k} & \text{at} \quad k \gg 1. \end{cases}$$

It should be noted that the analytic result, Eq. (13), reflects the fact that $\mathrm{Re}\,g_0(\varepsilon)$ is odd and $\mathrm{Im}\,g_0(\varepsilon)$ is even in energy (understood as $\varepsilon - i0$) in accordance with the particle–antiparticle symmetry. The respective DOS for a uniform *d*-wave SC crystal

$$\rho(\varepsilon) = \frac{1}{\pi}\mathrm{Im}\mathrm{Tr}\widehat{G}^0 = \frac{2}{\pi}\rho_N\,\mathrm{Im}\,g_0(\varepsilon)$$

displays sharp SC coherence peaks

$$\rho(\varepsilon) \approx \frac{2\rho_N}{\pi}\ln\left[4\sqrt{\left|1-(\Delta/\varepsilon)^2\right|}\right]$$

at $|\varepsilon| \to \Delta$, decays linearly as $\rho(\varepsilon) \approx |\varepsilon|\rho_N/\Delta$ at $|\varepsilon| \ll \Delta$, and tends to the normal state constant DOS value ρ_N at $|\varepsilon| \gg \Delta$ (Fig. 2).

The asymmetry factor beside $\hat{\tau}_3$ in Eq. (12) is almost constant:

$$g_{\mathrm{as}} = -\frac{1}{N}\sum_{\mathbf{k}}\frac{\xi_{\mathbf{k}}}{\varepsilon^2 - E^2_{\mathbf{k}}} \approx \ln\sqrt{W/\mu - 1}, \tag{14}$$

until $|\varepsilon| \ll \mu, W$ and only turns zero at exact half-filling, $\mu = W/2$. As will be seen below, this nonzero value is relevant for impurity perturbations on the *d*-wave spectrum.

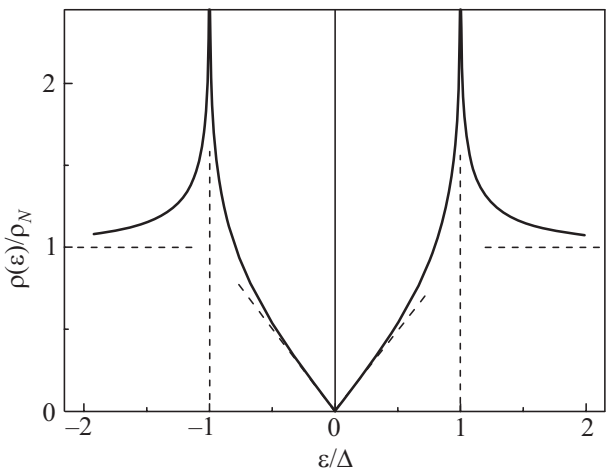

Fig. 2. DOS in a clean *d*-wave SC system (solid line). Dashed lines indicate the linear low-energy asymptotics, the logarithmic divergence at $|\varepsilon| \to \Delta$, and the tendency to constant value ρ_N at $|\varepsilon| \gg \Delta$.

Similarly, we can calculate the gap equation, Eq. (6), at $T \to 0$:

$$1 = \frac{V_{SC}\rho_N}{4\pi} \int\limits_0^{2\pi} d\varphi \int\limits_{-\varepsilon_D}^{\varepsilon_D} d\xi \frac{\cos^2 2\varphi}{\sqrt{\xi^2 + \Delta^2 \cos^2 2\varphi}}. \qquad (15)$$

Integrating this first in ξ, we have

$$\int\limits_{-\varepsilon_D}^{\varepsilon_D} \frac{d\xi}{\sqrt{\xi^2 + \Delta^2 \cos^2 2\varphi}} = 2\operatorname{arcsinh} \frac{\varepsilon_D}{\Delta |\cos 2\varphi|} =$$

$$\approx 2 \ln \frac{2\varepsilon_D}{\Delta |\cos 2\varphi|}$$

(since $\Delta \ll \varepsilon_D$). Doing next the angular integration

$$\int\limits_0^{2\pi} d\varphi \cos^2 2\varphi \ln \frac{2\varepsilon_D}{\Delta |\cos 2\varphi|} = \pi \left(\ln \frac{4\varepsilon_D}{\Delta} - \frac{1}{2} \right),$$

we arrive at the gap parameter

$$\Delta = 4\varepsilon_D e^{-1/\lambda - 1/2} \qquad (16)$$

with the dimensionless pairing constant $\lambda = V_{SC}\rho_N / 2$. As usually, this value can be compared with the critical temperature T_c of SC transition, found from the same gap equation, Eq. (5), under the condition $\Delta_{\mathbf{k}} \equiv 0$:

$$\frac{1}{\lambda} = \int\limits_0^{\varepsilon_D} \frac{d\xi}{\xi} \tanh \frac{\xi}{2k_B T_c} \approx \ln \frac{2\gamma_E \varepsilon_D}{\pi k_B T_c},$$

where $\gamma_E \approx 1.781$ is the Euler constant [49], so that

$$k_B T_c = (2\gamma_E \varepsilon_D / \pi) e^{-1/\lambda}. \qquad (17)$$

From comparison of Eqs. (16) and (17) we conclude that the characteristic ratio $r = 2\Delta / k_B T_c$ in this case is $2/\sqrt{e}$ times higher than the s-wave BCS value $r_{BCS} = 2\pi / \gamma_E \approx 3.52$, reaching $r \approx 4.27$. The above considered characteristics of the *d*-wave SC state in the pure crystal are essential for the impurity effects in the quasiparticle spectrum.

3.1. Impurity perturbation and group expansions

The simplest impurity perturbation of the Hamiltonian, Eq. (3), is realized by the point-like Lifshitz potential V_L on random lattice sites $\mathbf{p}$ with relative concentration $c \ll 1$. Its matrix form

$$H' = \frac{1}{N} \sum_{\mathbf{p},\mathbf{k},\mathbf{k}'} e^{i(\mathbf{k}-\mathbf{k}')\cdot\mathbf{p}} \psi^{\dagger}_{\mathbf{k}'} \hat{V} \psi_{\mathbf{k}} \qquad (18)$$

includes the impurity perturbation matrix $\hat{V} = V_L \hat{\tau}_3$. This is the most extensively used model for impurity effects in superconductors [4,15,36,50–52], but also some extensions of this form, either in spatial range of perturbed sites and in spin variables, are considered below.

In presence of impurities, the equation of motion for the Nambu matrix GF, related to the Hamiltonian $H + H'$ reads

$$\hat{G}_{\mathbf{k},\mathbf{k}'} = \delta_{\mathbf{k},\mathbf{k}'} \hat{G}^0_{\mathbf{k}} + \frac{1}{N} \sum_{\mathbf{p},\mathbf{k}''} e^{i(\mathbf{k}-\mathbf{k}'')\cdot\mathbf{p}} \hat{G}^0_{\mathbf{k}} \hat{V} \hat{G}_{\mathbf{k}'',\mathbf{k}'}, \qquad (19)$$

and we shall choose different routines to close the infinite chain of equations for the "scattered" GF's, like $\hat{G}_{\mathbf{k}'',\mathbf{k}'}$ in Eq. (19). In particular, the routine to obtain the above mentioned fully renormalized GE consists in consecutive iterations of this equation for the "scattered" GF's and in systematic separation of all those already present in the previous iterations [44]. It should be noted that the observable characteristics of a disordered system are described by the so-called *self-averaging* GF's, whose values for all particular realizations of disorder are practically nonrandom, equal to those averaged over disorder [26]. GE's are well defined just for self-averaging quantities, so one should always try to formulate each particular problem in terms of these quantities.

Thus, considering the m-diagonal $\hat{G}_{\mathbf{k}}$, the most important example of self-averaging GF, we separate, among the scattering terms, the function $G_{\mathbf{k}}$ itself from those with $\hat{G}_{\mathbf{k}',\mathbf{k}}$, $\mathbf{k}' \neq \mathbf{k}$:

$$\hat{G}_{\mathbf{k}} = \hat{G}^0_{\mathbf{k}} + \frac{1}{N} \sum_{\mathbf{k}',\mathbf{p}} e^{i(\mathbf{k}-\mathbf{k}')\cdot\mathbf{p}} \hat{G}^0_{\mathbf{k}} \hat{V} \hat{G}_{\mathbf{k}',\mathbf{k}} =$$

$$= \hat{G}^0_{\mathbf{k}} + c\hat{G}^0_{\mathbf{k}} \hat{V} G_{\mathbf{k}} + \frac{1}{N} \sum_{\mathbf{k}' \neq \mathbf{k},\mathbf{p}} e^{i(\mathbf{k}-\mathbf{k}')\cdot\mathbf{p}} \hat{G}^0_{\mathbf{k}} \hat{V} \hat{G}_{\mathbf{k}',\mathbf{k}}. \qquad (20)$$

Then for each $\hat{G}_{\mathbf{k}',\mathbf{k}}$, $\mathbf{k}' \neq \mathbf{k}$ we write down Eq. (19) again and single out the scattering terms with $\hat{G}_{\mathbf{k}}$ and $\hat{G}_{\mathbf{k}',\mathbf{k}}$ in its r.h.s.:

$$\hat{G}_{\mathbf{k}',\mathbf{k}} = \frac{1}{N} \sum_{\mathbf{k}'',\mathbf{p}'} e^{i(\mathbf{k}'-\mathbf{k}'')\cdot\mathbf{p}} \hat{G}^0_{\mathbf{k}'} \hat{V} \hat{G}_{\mathbf{k}'',\mathbf{k}} =$$

$$= c\hat{G}^0_{\mathbf{k}'} \hat{V} \hat{G}_{\mathbf{k}',\mathbf{k}} + \frac{1}{N} e^{i(\mathbf{k}'-\mathbf{k})\cdot\mathbf{p}} \hat{G}^0_{\mathbf{k}'} \hat{V} \hat{G}_{\mathbf{k}} +$$

$$+ \frac{1}{N} \sum_{\mathbf{p}' \neq \mathbf{p}} e^{i(\mathbf{k}'-\mathbf{k})\cdot\mathbf{p}'} \hat{G}^0_{\mathbf{k}'} \hat{V} \hat{G}_{\mathbf{k}} +$$

$$+ \frac{1}{N} \sum_{\mathbf{k}'' \neq \mathbf{k},\mathbf{k}';\mathbf{p}'} e^{i(\mathbf{k}'-\mathbf{k}'')\cdot\mathbf{p}'} \hat{G}^0_{\mathbf{k}'} \hat{V} \hat{G}_{\mathbf{k}'',\mathbf{k}}. \qquad (21)$$

Note that, among the terms with $\hat{G}_{\mathbf{k}}$, the $\mathbf{p}' = \mathbf{p}$ term (the second in r.h.s. of Eq. (21)) bears the phase factor $e^{i(\mathbf{k}'-\mathbf{k})\cdot\mathbf{p}}$, so it is coherent to that already present in the last sum in Eq. (20). That is why this term is explicitly separated from other, incoherent ones, $\propto e^{i(\mathbf{k}'-\mathbf{k})\cdot\mathbf{p}'}$, $\mathbf{p}' \neq \mathbf{p}$ (but there will be no such separation when doing 1st iteration of Eq. (19) for the m-nondiagonal GF $\hat{G}_{\mathbf{k}'',\mathbf{k}}$ itself).

Continuing the sequence, we collect the terms with the initial function $\hat{G}_{\mathbf{k}}$ which result from:

i) all multiple scatterings on the same site $\mathbf{p}$, and

ii) such processes on the same pair of sites $\mathbf{p}$ and $\mathbf{p}' \neq \mathbf{p}$, and so on.

Then summation in $\mathbf{p}$ of the i)-terms gives rise to the first term of GE as $c\hat{T}$, where

$$\hat{T} = \hat{V}(1 - \hat{G}\hat{V})^{-1}, \tag{22}$$

and, if the impurity cluster processes were neglected, this term would be just the self-consistent T-matrix [33,53]. The second term of GE, obtained by summation of the ii)-terms in $\mathbf{p}, \mathbf{p}' \neq \mathbf{p}$, contains the interaction matrices [15]

$$\hat{A}_{\mathbf{p}'-\mathbf{p}} = \frac{1}{N}\sum_{\mathbf{k}'} e^{i\mathbf{k}'\cdot(\mathbf{p}'-\mathbf{p})}\hat{G}_{\mathbf{k}'}\hat{T}$$

generated by the multiply scattered GF's $\hat{G}_{\mathbf{k}',\mathbf{k}}$, $\mathbf{k}' \neq \mathbf{k}$, etc. (including their own renormalization). For instance, the iterated equation of motion for $\hat{G}_{\mathbf{k}'',\mathbf{k}}$ with $\mathbf{k}'' \neq \mathbf{k}, \mathbf{k}'$ in the last term of Eq. (21) will produce

$$\hat{G}_{\mathbf{k}'',\mathbf{k}} = \frac{1}{N}\sum_{\mathbf{k}''',\mathbf{p}''} e^{i(\mathbf{k}''-\mathbf{k}''')\cdot\mathbf{p}''}\hat{G}^0_{\mathbf{k}''}\hat{V}\hat{G}_{\mathbf{k}''',\mathbf{k}} =$$

$$= \frac{1}{N}e^{i(\mathbf{k}''-\mathbf{k})\cdot\mathbf{p}}\hat{G}^0_{\mathbf{k}''}\hat{V}\hat{G}_{\mathbf{k}} + \frac{1}{N}e^{i(\mathbf{k}''-\mathbf{k})\cdot\mathbf{p}'}\hat{G}^0_{\mathbf{k}''}\hat{V}\hat{G}_{\mathbf{k}} +$$

$$+ \text{ terms with } \hat{G}_{\mathbf{k}',\mathbf{k}} \text{ and } \hat{G}_{\mathbf{k}'',\mathbf{k}} +$$

$$+ \text{ terms with } \hat{G}_{\mathbf{k}''',\mathbf{k}} \ (\mathbf{k}''' \neq \mathbf{k}, \mathbf{k}', \mathbf{k}''). \tag{23}$$

Finally we arrive at the fully renormalized representation for the m-diagonal GF as

$$\hat{G}_{\mathbf{k}} = \hat{G}_{\mathbf{k},\mathbf{k}} = \left[\left(\hat{G}^0_{\mathbf{k}}\right)^{-1} - \hat{\Sigma}_{\mathbf{k}}\right]^{-1}, \tag{24}$$

where the renormalized self-energy matrix is presented by the GE:

$$\hat{\Sigma}_{\mathbf{k}} = c\hat{T}\left(1 - c\hat{A}_0 - c\hat{A}_0^{\,2} + c\hat{B}_{\mathbf{k}} + \cdots\right). \tag{25}$$

Here the next to unity terms are due to quasiparticle scattering by impurity clusters, respectively to their c-orders. Thus, the c^2-terms result from impurity pairs, and the pair correlations define the term

$$\hat{B}_{\mathbf{k}} = \sum_{\mathbf{n}\neq 0}(\hat{A}^2_{\mathbf{n}}A_{-\mathbf{n}}e^{-i\mathbf{k}\cdot\mathbf{n}} + \hat{A}^2_{\mathbf{n}}A^2_{-\mathbf{n}})(1 - \hat{A}_{\mathbf{n}}\hat{A}_{-\mathbf{n}})^{-1}, \tag{26}$$

written so after replacing the sum in random impurity sites $\mathbf{p}'$ around a given $\mathbf{p}$, $\sum_{\mathbf{p}'\neq\mathbf{p}} f_{\mathbf{p}'-\mathbf{p}}$, by its positional average, $c\sum_{\mathbf{n}\neq 0} f_{\mathbf{n}}$, over all lattice sites around zero. The terms not written explicitly in Eq. (25) are due to the clusters of three and more impurities.

An alternative routine consists in iterations of the equation of motion for *all* the terms $\hat{G}_{\mathbf{k}'',\mathbf{k}}$ in Eq. (19) and summing the contributions $\propto \hat{G}^0_{\mathbf{k}}$, like the first term in the r.h.s. This finally leads to the solution of the form

$$\hat{G}_{\mathbf{k}} = \hat{G}^0_{\mathbf{k}} + \hat{G}^0_{\mathbf{k}}\hat{\Sigma}^0_{\mathbf{k}}\hat{G}^0_{\mathbf{k}}, \tag{27}$$

where the nonrenormalized self-energy

$$\hat{\Sigma}^0_{\mathbf{k}} = c\hat{T}^0(1 + c\hat{B}^0_{\mathbf{k}} + \cdots) \tag{28}$$

includes the nonrenormalized T-matrix

$$\hat{T}^0 = \hat{V}\left(1 - \hat{G}^0\hat{V}\right)^{-1}, \tag{29}$$

and the corresponding pair term:

$$\hat{B}^0_{\mathbf{k}} = \sum_{\mathbf{n}\neq 0}\left(\hat{A}^0_{\mathbf{n}}e^{-i\mathbf{k}\cdot\mathbf{n}} + \hat{A}^0_{\mathbf{n}}\hat{A}^0_{-\mathbf{n}}\right)\left(1 - \hat{A}^0_{\mathbf{n}}\hat{A}^0_{-\mathbf{n}}\right)^{-1}. \tag{30}$$

The nonrenormalized interaction matrices are given by

$$\hat{A}^0_{\mathbf{n}} = \hat{G}^0_{\mathbf{n}}\hat{T}^0, \quad \hat{G}^0_{\mathbf{n}} = \frac{1}{N}\sum_{\mathbf{k}} e^{i\mathbf{k}\cdot\mathbf{n}}\hat{G}^0_{\mathbf{k}}, \quad \hat{G}^0 \equiv \hat{G}^0_0. \tag{31}$$

Like the previous Eq. (25), the next to unity term in the brackets of Eq. (28) describes the contribution from all possible clusters of two impurities and the dropped terms are for clusters of three and more impurities. This permits to describe, in principle, the hierarchical structure of quasi-continuous spectrum of localized states in the crystal with impurities [26]. Besides the two above presented, other types of GE's (with different degrees of their renormalization) can be also obtained from specific routines for the equations of motion [54].

The crucial issue for group expansions is their convergence. Strictly speaking, it can be only asymptotic, moreover, it essentially depends on the chosen value of ε. In practice, we simply consider that the group series converges, at a given ε, if the contribution to the self-energy $\hat{\Sigma}$ from the 1st (single-impurity) term of GE dominates over that from the 2nd term (impurity pairs). Then it is believed that the pair term and all the rest of the series can be dropped, as is proved in some simplest model cases [45]. But with varying ε, a condition can be reached that the first two GE terms turn to be of the same order (and, supposedly, all the rest too), this is expected to define a limit of convergence for the given GE type. Such limits for different GE types are different [45], and we can combine between them to cover the maximum energy range. Finally, the areas of the spectrum where no GE is convergent define special regions, like the regions of concentration broadening around localized levels or the mobility edges (dividing band-like states from localized states). The quantitative analysis of GE convergence and of impurity cluster effects begins from the simplest single-impurity level, providing the elements for all the following steps.

4. Impurity effects on superconducting state

Using Eqs. (12), (29), we express the nonrenormalized T-matrix as

$$\hat{T}^0(\varepsilon) = \frac{v}{\rho_N}\frac{vg_0 - \hat{\tau}_3}{1 - v^2 g_0^2}, \tag{32}$$

through the function $g_0(\varepsilon)$, Eq. (13), and the dimensionless perturbation parameter $v = V_L\rho_N / \left(1 - V_L\rho_N g_{as}\right)^{-1}$ [55]. This T-matrix permits existence of low-energy resonances [14,15] at symmetric points $\varepsilon = \pm\varepsilon_{res}$, found from the condition $\mathrm{Re}[vg_0(\varepsilon_{res})]^2 = 1$, analogous to the known Lifshitz equation in normal metals and semiconductors [26].

Since $\mathrm{Re}[g_0(\varepsilon)]^2 \approx [\mathrm{Im\,K}(\Delta^2/\varepsilon^2)]^2 - [\mathrm{Re\,K}(\Delta^2/\varepsilon^2)]^2$ reaches its highest value ≈ 0.47 at $|\varepsilon| \approx 0.443\Delta$, the formal solution to the Lifshitz equation first appears just at these points when the perturbation v reaches ≈ 1.46. However, this formal solution will not yet correspond to a true resonance peak in DOS because its broadening $\Gamma_{res} \approx \mathrm{Im}\, g_0(\varepsilon_{res}) / (d\mathrm{Re}\, g_0 / d\varepsilon)_{\varepsilon_{res}}$ reaches $\approx 0.541\Delta$ in this case, that is larger of ε_{res} itself. But for strong enough perturbation: $v \gg 1$, the resonance energy is low, $\varepsilon_{res} \ll \Delta$, and from the logarithmic asymptotics: $\mathrm{Re}\, g_0(\varepsilon) \approx (\varepsilon/\Delta)\ln(4\Delta/\varepsilon)$, it estimates as $\varepsilon_{res} \approx \Delta/[v\ln(4v)]$ [14,15]. Then also the broadening $\Gamma_{res} \approx \pi\varepsilon_{res}/[2\ln(4v)]$ is smaller than ε_{res} (though not very much) already for $v \gtrsim 1.7$, as seen in Fig. 3.

It is important to notice that in presence of the finite asymmetry factor g_{as}, Eq. (14), the perturbation parameter can be very large, $|v| \gg 1$, even for a moderate perturbation potential $V_L \sim 1/\rho_N$ if $V_L\rho_N g_{as}$ gets close to unity. This can open possibility for the unitary scattering regime [36] in superconductors with rather common impurity substitutes as transition metals or Zn for Cu. This specific property of impurity scattering in high-T_c systems with asymmetric bands was first indicated by Hirschfeld *et al.* [56].

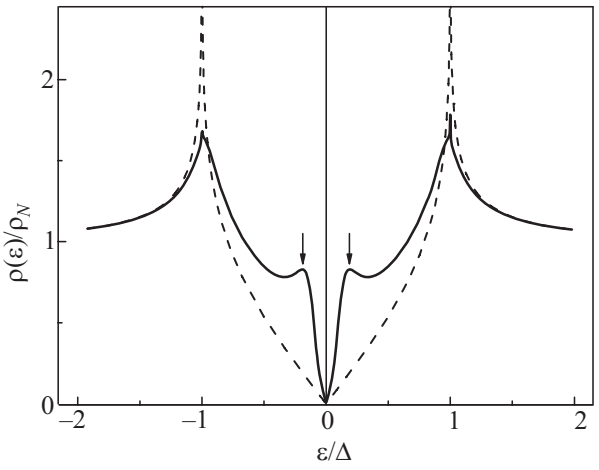

Fig. 3. Low-energy resonance levels $\pm\varepsilon_{res}$ (arrows) in the DOS of *d*-wave superconductor containing a finite concentration $c = 0.2\rho_N\Delta$ of impurity scatterers with $V_L \approx 0.67/\rho_N$ (corresponding to $v \approx 2$). Other distinctions from the pure crystal DOS in Fig. 2 (shown here by the dashed line) are the finite spikes at $|\varepsilon| = \Delta$ and the enhanced slope at $|\varepsilon| < \varepsilon_{res}$.

The local SC order parameter in the *d*-wave system is constructed from the off-diagonal correlators between nearest neighbor sites in the lattice, $\left\langle a_{\mathbf{n}+\boldsymbol{\delta},\uparrow} a_{\mathbf{n},\downarrow} \right\rangle$, where $\boldsymbol{\delta} = (\pm a/2, \pm a/2)$, taking the GF form (in agreement with Eq. (2))

$$\Delta_{\mathbf{n}} = \frac{V_{SC}}{2\pi N}\sum_{\mathbf{k},\mathbf{k}'} e^{i[\mathbf{k}\cdot(\mathbf{n}+\boldsymbol{\delta}) - \mathbf{k}'\cdot\mathbf{n}]}\theta(\varepsilon_D^2 - \xi_{\mathbf{k}}^2)\theta(\varepsilon_D^2 - \xi_{\mathbf{k}'}^2)\times$$

$$\times \int_{-\infty}^{\infty} \frac{d\varepsilon}{e^{\varepsilon/T}+1}\,\mathrm{Im\,Tr}\,\widehat{G}_{\mathbf{k},\mathbf{k}'}\hat{\tau}_1. \tag{33}$$

Its average value over all the sites **n** is presented in the GF form as

$$\Delta = \frac{V_{SC}}{2\pi}\int_{-\infty}^{\infty}\frac{d\varepsilon}{e^{\varepsilon/T}+1}\,\mathrm{Im\,Tr}\,\widehat{F}^0_{\boldsymbol{\delta}}\hat{\tau}_1. \tag{34}$$

Here the elements of the matrix

$$\widehat{F}^0_{\boldsymbol{\delta}} = \frac{1}{N}\sum_{\mathbf{k}} e^{i\mathbf{k}\cdot\boldsymbol{\delta}}\theta(\varepsilon_D^2 - \xi_{\mathbf{k}}^2)\widehat{G}^0_{\mathbf{k}} \tag{35}$$

are calculated accordingly to the rules

$$\sum_{\mathbf{k}} f(k) e^{i\mathbf{k}\cdot\boldsymbol{\delta}} \approx \sum_k f(k),$$

$$\sum_{\mathbf{k}} f(k) e^{i\mathbf{k}\cdot\boldsymbol{\delta}} \cos 2\varphi_{\mathbf{k}} \approx \frac{\pi\mu\rho_N}{2}\sum_{\mathbf{k}} f(k)\cos^2 2\varphi_{\mathbf{k}},$$

$$\sum_{\mathbf{k}} \xi_{\mathbf{k}}\theta(\varepsilon_D^2 - \xi_{\mathbf{k}}^2) f(\xi_{\mathbf{k}}^2) = 0,$$

to result in

$$\widehat{F}^0_{\boldsymbol{\delta}} \approx \rho_N\left(f_0 + \frac{\pi\mu\rho_N}{2} g_1 \hat{\tau}_1\right). \tag{36}$$

This includes another energy function

$$g_1(\varepsilon) = \frac{\Delta}{2\pi}\int_0^{2\pi}\cos^2 2\varphi\, d\varphi \int_0^{\varepsilon_D}\frac{d\xi}{\varepsilon^2 - \xi^2 - \Delta^2\cos^2 2\varphi} \approx$$

$$\approx \frac{\Delta}{2\varepsilon_D} - i\frac{\varepsilon}{\Delta}\left[\mathrm{K}\left(\frac{\Delta^2}{\varepsilon^2}\right) - \mathrm{E}\left(\frac{\Delta^2}{\varepsilon^2}\right)\right],$$

with the full elliptic integral of 2nd kind E [49], and the function f_0 which only differs from g_0, Eq. (12), by its last term being $\varepsilon/\varepsilon_D$. Absence of asymmetry term $\propto \hat{\tau}_3$ in Eq. (36) is due to the BCS shell factor $\theta(\varepsilon_D^2 - \xi_{\mathbf{k}}^2)$ present in Eq. (35).

The local deviation of SC order parameter $\Delta_{\mathbf{n}}$ on **n**th site from its average value Δ is only defined by the m-nondiagonal contributions into Eq. (33), which are easily calculated for the simplest case of a single impurity center at $\mathbf{p} = 0$:

$$\hat{G}_{\mathbf{k},\mathbf{k}'} = \frac{1}{N}\hat{G}^0_{\mathbf{k}}\hat{T}^0\hat{G}^0_{\mathbf{k}'}, \tag{37}$$

expressing this variation in terms of matrices $\hat{F}$ as

$$\Delta_{\mathbf{n}} - \Delta = \frac{V_{SC}}{2\pi}\int\limits_{-\infty}^{\infty}\frac{d\varepsilon}{e^{\varepsilon/T}+1}\,\mathrm{Im}\,\mathrm{Tr}\,\hat{F}^0_{\mathbf{n}+\boldsymbol{\delta}}\hat{T}^0\hat{F}^0_{\mathbf{n}}\hat{\tau}_1. \tag{38}$$

Taking into account that $\hat{F}^0_0$ is simply a scalar $\rho_N f_0$ and considering zero temperature, we obtain the parameter $\eta = 1 - \Delta_0/\Delta$ of relative suppression of SC order on the very impurity site $\mathbf{n} = 0$ in the form

$$\eta = -\frac{\int\limits_0^{\varepsilon_D} d\varepsilon\,\mathrm{Im}\mathrm{Tr}\,\hat{F}^0_{\boldsymbol{\delta}}\hat{T}^0\hat{F}^0_0\hat{\tau}_1}{\int\limits_0^{\varepsilon_D} d\varepsilon\,\mathrm{Im}\mathrm{Tr}\,\hat{F}^0_{\boldsymbol{\delta}}\hat{\tau}_1} =$$

$$= -\frac{v^2\int\limits_0^{\varepsilon_D} d\varepsilon\,\mathrm{Im}\left[g_0 f_0 g_1/(1-v^2 g_0^2)\right]}{\int\limits_0^{\varepsilon_D} d\varepsilon\,\mathrm{Im}\,g_1}, \tag{39}$$

as a function of the perturbation parameter v. This numerically calculated function $\eta(v)$, when compared to the analytic result for impurity in an *s*-wave superconductor [15]: $\eta_s(v) = \pi^2 v^2/(1+\pi^2 v^2)$, presents a sensible delay of its growth with v (Fig. 4). This is apparently due to the pronounced negative effect of the low-energy resonance level $\varepsilon_{\mathrm{res}}$ on the integrand function in numerator of Eq. (37), compared to the integrand in its denominator (inset in Fig. 4), whereas in the *s*-wave case, at absence of impurity resonance, the two integrands (in numerator and denominator) are simply proportional to each other.

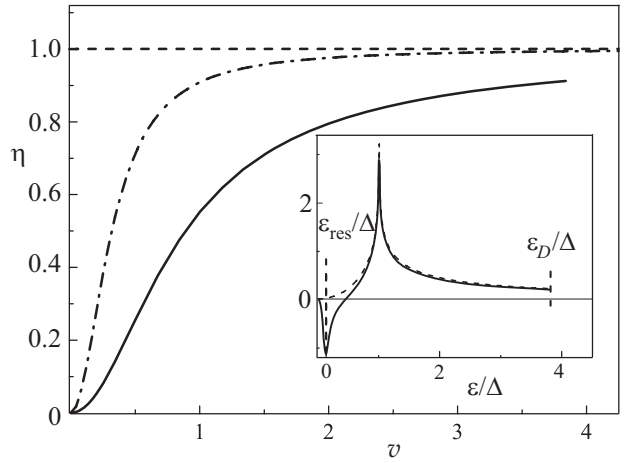

Fig. 4. Suppression of the local SC order parameter at the very impurity site $\eta = 1 - \Delta_0/\Delta$ in function of the perturbation parameter v, calculated for *d*-wave case from Eq. (39) (solid line) vs its analytical *s*-wave form $\pi^2 v^2/(1+\pi^2 v^2)$ [15] (dash-dotted line). Inset: comparison of the integrand functions in the numerator (solid line) and denominator (dashed line) of Eq. (39) at $v = 2$ reveals a notable negative effect of the resonance level at $\varepsilon_{\mathrm{res}}$ that diminishes η in the *d*-wave case vs the *s*-wave case where no such resonance exist.

5. Other types of impurity centers

5.1. Extended impurity center

The predicted effects of a point-like scatterer on the local SC order are perhaps too strong to be adequate to the observed stability of SC state under disorder. In reality the impurity perturbations in high-T_c materials are not exactly point-like but rather extended to a finite number of neighbor sites to the impurity center. This raises an important question on how robust are the results of a point-like model with respect to the spatial extent and geometry of impurity perturbation. The opposite limit to the point-like perturbation, that when the defect is much bigger of the Fermi wavelength and can be treated quasiclassically [57], hardly applies to real atomic substitutes in high-T_c systems with perturbation limited to few nearest neighbors of the impurity site. To model the latter situation, we extend the perturbation Hamiltonian, Eq. (18), to the form [58]

$$H_{\mathrm{ext}} = -\frac{1}{N}\sum_{\mathbf{k},\mathbf{k}',\mathbf{p}} e^{i(\mathbf{k}'-\mathbf{k})\cdot\mathbf{p}}\sum_{\boldsymbol{\delta}} e^{i(\mathbf{k}'-\mathbf{k})\cdot\boldsymbol{\delta}}\Psi^{\dagger}_{\mathbf{k}'}\hat{V}\Psi_{\mathbf{k}}. \tag{40}$$

It contains formally the same perturbation matrix $\hat{V} = V_L\hat{\tau}_3$ as in Eq. (18), but takes an explicit account of the phase shifts $e^{i(\mathbf{k}'-\mathbf{k})\cdot\boldsymbol{\delta}}$ at quasiparticle scattering by extended perturbation on the nearest neighbor lattice sites $\boldsymbol{\delta}$ to the impurity center **p** (which itself does not pertain to the lattice in this case, see Fig. 5). Then the equation of motion, Eq. (19), is modified to

$$\hat{G}_{\mathbf{k},\mathbf{k}'} = \hat{G}^0_{\mathbf{k}}\delta_{\mathbf{k},\mathbf{k}'} + \frac{1}{N}\sum_{\mathbf{k}'',\mathbf{p},j} e^{i(\mathbf{k}-\mathbf{k}'')\cdot\mathbf{p}}\alpha_{j,\mathbf{k}}\alpha_{j,\mathbf{k}''}\hat{G}^0_{\mathbf{k}}\hat{V}\hat{G}_{\mathbf{k}'',\mathbf{k}'}, \tag{41}$$

where the functions

$$\alpha_{1,\mathbf{k}} = 2\cos\frac{ak_x}{2}\cos\frac{ak_y}{2},$$

$$\alpha_{2,\mathbf{k}} = 2\cos\frac{ak_x}{2}\sin\frac{ak_y}{2},$$

$$\alpha_{3,\mathbf{k}} = 2\sin\frac{ak_x}{2}\cos\frac{ak_y}{2},$$

$$\alpha_{4,\mathbf{k}} = 2\sin\frac{ak_x}{2}\sin\frac{ak_y}{2}, \tag{42}$$

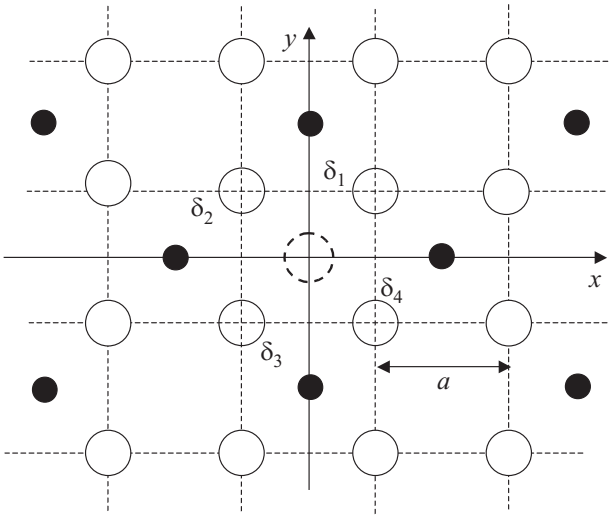

Fig. 5. Extended perturbation over four nearest oxygen sites δ_i to the impurity ion (its projection onto the CuO_2 plane is shown by the dashed circle at the origin).

realize irreducible representations of the C_4 point group ($j = 1$ being related to *A*-, $j = 2,3$ to *E*-, and $j = 4$ to *B*-representations [59]) and thus satisfy the orthogonality condition

$$\frac{1}{N}\sum_{\mathbf{k}}\alpha_{j,\mathbf{k}}\alpha_{j',\mathbf{k}} = \delta_{j,j'}. \tag{43}$$

The impurity effects on quasiparticle spectrum are naturally classified along these representations, alike the known effects of magnetic impurities in ferro- and antiferromagnetic crystals [45,60].

Orthogonality of the $\alpha_{j,\mathbf{k}}$ functions results in that Eq. (41) has a solution formally coinciding with Eq. (27), but with the T-matrix additive in the C_4 representations: $\hat{T}^0 = \sum_j \hat{T}^0_j$, where each partial T-matrix $\hat{T}^0_j = \hat{V}(1-\hat{G}^0_j\hat{V})^{-1}$ includes the specific local GF matrix: $\hat{G}^0_j = N^{-1}\sum_{\mathbf{k}}\alpha^2_{j,\mathbf{k}}\hat{G}^0_{\mathbf{k}}$. Alike Eq. (32), this matrix can be expanded in the basis of Pauli matrices

$$\hat{G}^0_j = \rho_N(g_{j0} + g_{j1}\hat{\tau}_1 - g_{j3}\hat{\tau}_3). \tag{44}$$

The functions g_{ji} are calculated by using Eq. (10), some of them are zero by the symmetry reasons: $g_{11} = g_{41} = 0$, and the rest can be approximated as

$$g_{j0} \approx \overline{\alpha^2_j} g_0, \quad g_{j3} \approx \overline{\alpha^2_j} g_{\mathrm{as}}, \quad g_{21} = -g_{31} \approx \overline{\alpha^2_2} g_1. \tag{45}$$

Here $\overline{\alpha^2_j}$ are the average values of $\alpha^2_{j,\mathbf{k}}$ over the Fermi surface: $\overline{\alpha^2_1} \approx 4(1-\mu/W)$, $\overline{\alpha^2_{2,3}} \approx 4\mu/W$, $\overline{\alpha^2_4} \approx 2(\mu/W)^2$, where the band occupation parameter μ/W is supposedly small. Then the most important contribution to $\hat{T}^0$ comes from the $j = 1$ term (*A*-representation):

$$\hat{T}^0_1 = \frac{v_A}{\overline{\alpha^2_1}\rho_N}\frac{v_A g_0 - \hat{\tau}_3}{D_A}, \tag{46}$$

with the *A*-channel perturbation parameter $v_A = \overline{\alpha^2_1} V_L \rho_N / (1 - \overline{\alpha^2_1} V_L \rho_N g_{\mathrm{as}})$ and the denominator $D_A(\varepsilon) = 1 - v_A^2 g_0^2(\varepsilon)$. It can produce low-energy resonances at $\varepsilon = \pm\varepsilon_{\mathrm{res}}$ (such that $\mathrm{Re}\, D_A(\varepsilon_{\mathrm{res}}) = 0$), similar to the above mentioned resonances for point-like impurity center. This again requires that v_A exceeds a critical value $v_{A,\mathrm{cr}} \approx 2/\pi$.

The contributions from $j = 2,3$ (*E*-representation) are

$$\hat{T}^0_{2,3} = \frac{v_E}{\overline{\alpha^2_2}\rho_N}\frac{v_E(g_0 \mp g_1\hat{\tau}_1) - \hat{\tau}_3}{D_E}, \tag{47}$$

with

$$v_E = \overline{\alpha^2_2} V_L \rho_N / (1 - \overline{\alpha^2_2} V_L \rho_N g_{\mathrm{as}}), \quad D_E = 1 - v_E^2(g_0^2 - g_1^2).$$

It is less probable to have a resonance effect in this channel at low occupation $\mu/W \ll 1$, since the reduced parameter v_E compared to v_A and competition between $\mathrm{Re}\, g_0^2$ and $\mathrm{Re}\, g_1^2$ in D_E.

The *B*-channel $\hat{T}^0_4$ has the same structure as the *A*-channel term, Eq. (48), but with v_A replaced by a strongly reduced value

$$v_B = \overline{\alpha^2_4} V_L \rho_N / (1 - \overline{\alpha^2_4} V_L \rho_N g_{\mathrm{as}}),$$

hence it turns even less important than the *E*-channel terms.

Now, using Eqs. (46), (47) in Eq. (8), the global DOS is obtained as

$$\rho(\varepsilon) \approx \frac{\rho_N}{\pi}\,\mathrm{Im}\, g_0(\varepsilon - \Sigma_0), \tag{48}$$

where the scalar self-energy

$$\Sigma_0 = \frac{\pi c W g_0(\varepsilon)}{4}\left(\frac{v_A^2}{\overline{\alpha^2_1} D_A} + \frac{2v_E^2}{\overline{\alpha^2_2} D_E} + \frac{v_B^2}{\overline{\alpha^2_4} D_B}\right) \tag{49}$$

includes the effects of all three channels. Figure 6 presents the results of direct calculation from Eq. (48) with use of Eq. (49) at a typical choice of parameters, $W = 2$ eV, $\mu = 0.3$ eV, $\varepsilon_D = 0.15$ eV, $V_L = 0.3$ eV (this gives for particular channels: $v_A \approx 1.763$, $v_E \approx 0.129$, and $v_B \approx 0.009$), and $c = 0.1$. They are similar to the results for point-like impurities [4,15], showing low-energy resonances at $\pm\varepsilon_{\mathrm{res}}$, mainly due to the *A*-channel effect. But the reduction of coherence peaks at $|\varepsilon| = \Delta$ is much stronger, due to additional effect from the *E*-channel, while the *B*-channel has no appreciable effect at all.

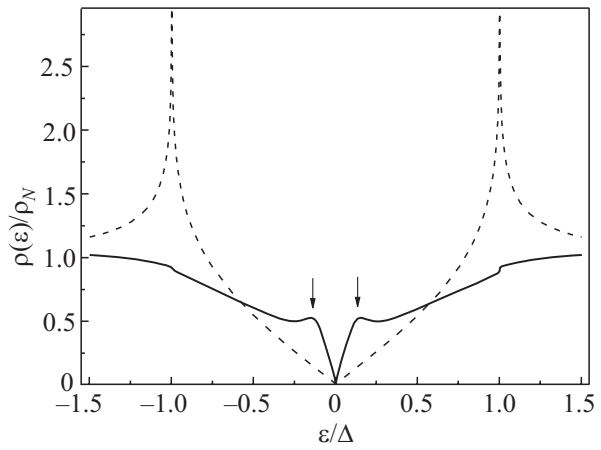

Fig. 6. DOS in the *d*-wave superconductor with extended impurity centers (the solid line), for the choice of parameters $W = 2$ eV, $\mu = 0.3$ eV, $\varepsilon_D = 0.15$ eV, $V_L = 0.3$ eV, $c = 0.1$. The arrow indicates the low-energy resonance by the *A*-channel impurity effect and the dashed line represents the pure *d*-wave DOS.

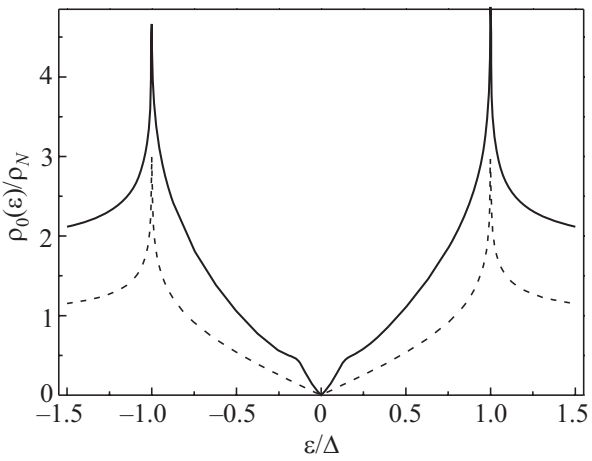

Fig. 7. Local density of states on the nearest neighbor site to an extended impurity center, for the same choice of parameters as in Fig. 6 (but supposing $c \to 0$). Note the overall enhancement of electronic density compared to that on remote sites from impurity (dashed line).

In analogy with Eq. (38) for the variation of SC order parameter, the variation of LDOS $\rho_n(\varepsilon)$, Eq. (10), near the impurity site, compared to the average value $\rho(\varepsilon)$, is only given by the m-nondiagonal GF's:

$$\delta\rho_{\mathbf{n}}(\varepsilon) = \frac{1}{\pi N}\sum_{\mathbf{k},\mathbf{k}'\neq\mathbf{k}} e^{i(\mathbf{k}-\mathbf{k}')\cdot\mathbf{n}}\,\mathrm{Im}\mathrm{Tr}\,\hat{G}_{\mathbf{k},\mathbf{k}'}. \qquad (50)$$

Here $\hat{G}_{\mathbf{k},\mathbf{k}'} = N^{-1}\sum_j \alpha_{j,\mathbf{k}}\hat{G}^0_{\mathbf{k}}\hat{T}^0_j\hat{G}^0_{\mathbf{k}'}\alpha_{j,\mathbf{k}'}$, and the strongest variation is attained at $\mathbf{n} = \boldsymbol{\delta}$, the nearest neighbor sites to the impurity. Using Eq. (50) and the orthogonality relations, we expand this value into a sum

$$\delta\rho_{\mathbf{n}=\boldsymbol{\delta}}(\varepsilon) = \frac{1}{\pi N^2}\sum_{\mathbf{k},\mathbf{k}',j} e^{i(\mathbf{k}-\mathbf{k}')\cdot\boldsymbol{\delta}}\,\mathrm{Im}\mathrm{Tr}\,\alpha_{j,\mathbf{k}}\hat{G}^0_{\mathbf{k}}\hat{T}^0_j\hat{G}^0_{\mathbf{k}'}\alpha_{j,\mathbf{k}'} =$$

$$= \frac{1}{\pi}\sum_j \mathrm{Im}\mathrm{Tr}\hat{G}^0_j\hat{T}^0_j\hat{G}^0_j,$$

and present the overall maximum LDOS as

$$\rho_{\mathbf{n}=\boldsymbol{\delta}}(\varepsilon) = \frac{2\rho_N}{\pi}\,\mathrm{Im}\left[g_0(\varepsilon)\left(1 + \frac{v_A N_A}{\alpha_1^2 D_A} + 2\frac{v_E N_E}{\alpha_2^2 D_E} + \frac{v_B N_B}{\alpha_4^2 D_B}\right)\right]. \qquad (51)$$

Alike Eq. (48) for global DOS, the resonance contribution to Eq. (51) at low energies $\varepsilon \sim \varepsilon_{\mathrm{res}}$ comes from the *A*-term with the numerator $N_A = 2g_3 + v_A(g_0^2 + g_3^2)$. Other channels, with $N_E = 2g_3 + v_E(g_0^2 - g_1^2 - g_3^2)$ and $N_B = 2g_3 + v_B(g_0^2 + g_3^2)$, mainly contribute to modification of the pure *d*-wave DOS $\rho_d(\varepsilon) = 2/[\pi\mathrm{Im}\,g_0(\varepsilon)]$ far from the resonance. LDOS on nearest neighbor sites to the impurity, calculated from Eq. (51) (solid line in Fig. 7), displays less pronounced low-energy resonances than those in the global DOS, Fig. 6, but an overall enhancement compared to the LDOS curve for remote sites from impurity $\rho_{\mathbf{n}\to\infty}(\varepsilon) = \rho(\varepsilon)$ (the dashed line). This picture resembles the direct experimental measurements of differential conductance through the STM tip positioned close to and far from an impurity center [18].

Similarly, the local perturbation of SC order parameter, Eq. (38), can be considered. The local *d*-wave SC order in the unit cell containing the impurity (see Fig. 5) is given by the average $\Delta_{\mathbf{n}} = V_{SC}\langle a_{\mathbf{n}+\boldsymbol{\delta}_1,\downarrow}a_{\mathbf{n}+\boldsymbol{\delta}_2,\uparrow}\rangle$ (of course, any pair of nearest neighbor sites to impurity can be chosen instead of $\boldsymbol{\delta}_1$ and $\boldsymbol{\delta}_2$). Again, the suppression parameter for this extended defect is defined as $\eta_{\mathrm{ext}} = 1 - \Delta_0/\Delta$, and it is only contributed by the nondiagonal GF's:

$$\eta_{\mathrm{ext}} = -\frac{V_{SC}W}{4\mu N\Delta}\sum_{\mathbf{k},\mathbf{k}''\neq\mathbf{k}} e^{i(\mathbf{k}\cdot\boldsymbol{\delta}_2 - \mathbf{k}'\cdot\boldsymbol{\delta}_3)}\theta(\varepsilon_D^2 - \xi_{\mathbf{k}}^2)\times$$

$$\times\,\theta(\varepsilon_D^2 - \xi_{\mathbf{k}'}^2)\langle a_{-\mathbf{k},\downarrow}a_{\mathbf{k}',\uparrow}\rangle =$$

$$= -\frac{\sum_j (-1)^j \int_{-\infty}^{0} d\varepsilon\,\mathrm{Im}\mathrm{Tr}\hat{F}^0_j\hat{T}^0_j\hat{F}^0_j\hat{\tau}_1}{\int_{-\infty}^{0} d\varepsilon\,\mathrm{Im}\mathrm{Tr}\hat{F}^0_{\boldsymbol{\delta}}\hat{\tau}_1}, \qquad (52)$$

where the matrices

$$\hat{F}^0_j = N^{-1}\sum_{\mathbf{k}}\alpha^2_{j,\mathbf{k}}\theta(\varepsilon_D^2 - \xi_{\mathbf{k}}^2)\hat{G}^{(0)}_{\mathbf{k}}$$

mainly differ from $\hat{G}^0_j$ by the absence of $\propto\hat{\tau}_3$ term, like in Eq. (36) which again defines $\hat{F}^0_{\boldsymbol{\delta}}$. Using here Eqs. (52), (44), one arrives at the expression

$$\eta_{\mathrm{ext}} = -2v_E^2\,\frac{\int_0^{\varepsilon_D}\mathrm{Im}\left[g_1(2f_0g_0 + f_0^2 + g_1^2)/D_E\right]d\varepsilon}{\int_0^{\varepsilon_D}\mathrm{Im}\,g_1(\varepsilon)d\varepsilon}, \qquad (53)$$

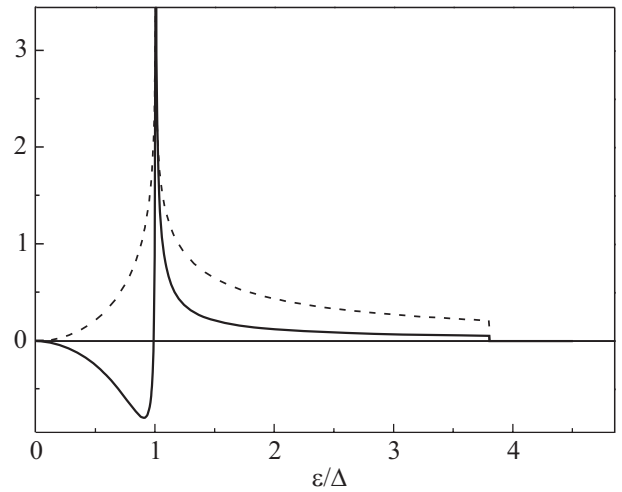

Fig. 8. The dimensionless function $F(\varepsilon)$ (solid line) used in the numerator of Eq. (52), compared to the dimensionless integrand in its denominator (dashed line) to calculate the suppression parameter η_{sup} at the same conditions as in Fig. 4.

where only the *E*-channel terms contribute to the numerator (see Fig. 8 to compare it with the denominator).

Numeric analysis of this expression for the above chosen perturbation parameters results in $\eta_{\text{ext}} \approx 0.132$. This value is much smaller than that for the point-like impurity (assuming $v = v_A$ gives $\eta \approx 0.763$), and, in view of the said in the beginning of this Section, the present model looks more plausible for disordered high-T_c systems. The most evident physical reason for so weak suppression is the separate action of the extended impurity center in different symmetry channels, so that the stronger perturbation, v_A, is effective for the N-diagonal characteristics (DOS and LDOS) while the N-nondiagonal ones (as SC order) are defined only by the weak perturbation, v_E. As will be shown below, even more diverse effects on local DOS and *d*-wave order parameter are produced by the extended impurity perturbation if it is spin-dependent.

5.2. Magnetic perturbation from nonmagnetic impurity

Unlike the above mentioned distinct effects of magnetic and nonmagnetic impurities in traditional SC materials, introduction of nonmagnetic Zn^{2+} ions instead of Cu^{2+} into the cuprate planes has a suppression effect on HTSC, not weaker but rather stronger than that by true magnetic ions, as Ni^{2+} [13]. Therefore nonmagnetic impurity ions in HTSC are seen as extremely strong scatterers [61], treated in the unitary limit [36,62,63]. However, the impurity centers formed in the CuO_2 plane by *homovalent* substitution (as Zn^{2+} or Ni^{2+} for Cu^{2+}), hardly could produce so strong perturbation potential. Also the predicted symmetric resonances by nonmagnetic impurities in LDOS are not observed in the experimental STM spectra taken near Zn sites in $Bi_2Sr_2CaCu_2O_{8+\delta}$ [18].

This Section presents an alternative approach to the problem of Cu-substituting impurities. It will be shown that, irrespectively of their type (magnetic or nonmagnetic), the resulting center generally acts on charge carriers as *magnetic*. In accordance with the general concept of time-reversal symmetry breaking, such center should in fact strongly suppress SC order either of *s*- or *d*-type, as was first qualitatively stated yet by Mahajan *et al.* [64]. Similar views on the effect of Zn impurities in high-T_c cuprates were expressed more recently [65–67], though still focusing on unitary scattering. As seen below, the spin-dependent effect of isolated (nonmagnetic) impurity in a CuO_2 plane, not reaching the unitary limit of perturbation but changing its Nambu structure, can become really strong [68].

Figure 9 shows a cathion impurity substitute for Cu in a CuO_2 plane, like real Zn, Fe, or Ni impurities in high-T_c compounds, and this center presents a notable geometric similarity to the extended center, Fig. 5 from the previous Section. However, there is also a difference in the mechanism of perturbation by these two centers. The main perturbation on O^- holes by the present type of impurity (regardless of being magnetic or nonmagnetic) is due to the fact that its neighbor O sites occur in a nonzero exchange field by Cu^{2+} spins [69,70], which is equivalent to the effect of magnetic impurity in a common superconductor. On the other hand, there are no reasons to consider any sizeable spin-independent perturbation from such isovalent impurity.

The respective model Hamiltonian consists in three terms: $H + H_c + H_{\text{int}}$, where H is given by Eq. (3). The first perturbation term $H_c = -hS_z$ models the (AFM) correlation between the impurity center and its environment,

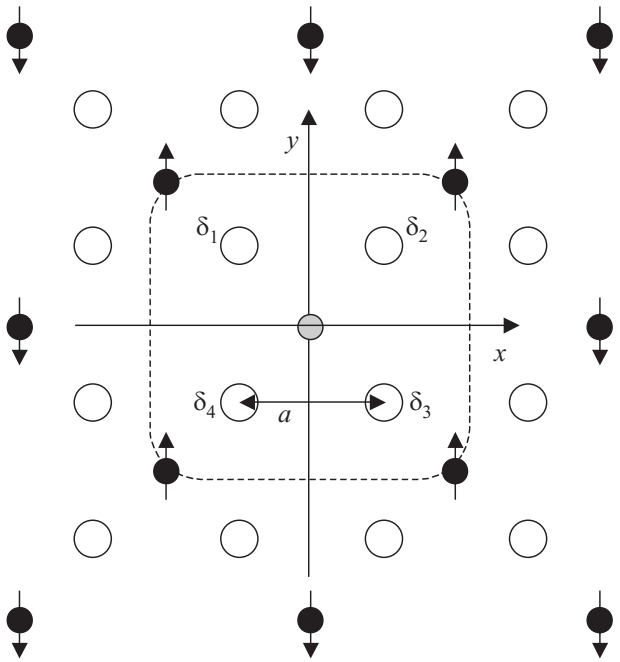

Fig. 9. Effective magnetic perturbation for charge carriers on nearest neighbor sites to the nonmagnetic impurity substitute for Cu^{2+} in CuO_2 plane.

where $h \sim J_{dd}$ is the Cu–Cu exchange constant and **S** is the spin of a fictitious "magnetic impurity". It can be attributed to the cluster of four 1/2 spins of Cu nearest neighbors to real nonmagnetic impurity. In reality, its quantization axis z is only defined over time periods no longer than $\tau_s \sim \hbar\xi_s/(aJ_{dd}) \sim 10^{-13}$ s for experimentally measured spin correlation length $\xi_s \sim a/\sqrt{x}$ [71] and doping levels $x \sim 0.1$ (this also agrees with the NMR data [65]). However τ_s is much longer than typical electronic times $\sim \hbar/\mu \sim 10^{-15}$ s for HTSC compounds. For $h > 0$ we have $\langle S_z \rangle \equiv s$ and $0 < s < S$, which accounts for the short-range AFM order, whereas $s \to 0$ in the paramagnetic limit $h \ll k_B T$. The spin-dependent interaction between charge carriers and impurity is can be also separated into three parts:

$$H_{\rm int} = H_{\rm int}^{MF} + H_{\rm int}^{\parallel} + H_{\rm int}^{\perp}, \tag{54}$$

where

$$H_{\rm int}^{MF} = \frac{Js}{N} \sum_{\mathbf{k},\mathbf{k}'} \sum_{\sigma=\pm} \alpha_{j,\mathbf{k}} \alpha_{j,\mathbf{k}'} \sigma a^{\dagger}_{\mathbf{k}',\sigma} a_{-\mathbf{k},\sigma}$$

describes the "mean-field" (MF) polarization of carrier spins by the impurity center, and

$$H_{\rm int}^{\parallel} = \frac{J}{N} \sum_{\mathbf{k},\mathbf{k}'} \sum_{\sigma=\pm} \alpha_{j,\mathbf{k}} \alpha_{j,\mathbf{k}'} \sigma (S_z - s) a^{\dagger}_{\mathbf{k}',\sigma} a_{\mathbf{k},\sigma},$$

$$H_{\rm int}^{\perp} = \frac{J}{N} \sum_{\mathbf{k},\mathbf{k}'} \sum_{\sigma=\pm} \alpha_{j,\mathbf{k}} \alpha_{j,\mathbf{k}'} S_{\sigma} a^{\dagger}_{\mathbf{k}',-\sigma} a_{\mathbf{k},\sigma},$$

are their interactions with longitudinal and transversal fluctuations of **S**. In the paramagnetic limit, $s \to 0$, Eq. (54) is reduced to the common Kondo interaction [72,73]. For definiteness, the Cu–O p–d exchange parameter J is taken positive. The functions $\alpha_{j,\mathbf{k}}$ are formally the same as given by Eq. (42) for extended impurity center in the previous Section, but the distinctive features of the perturbation, Eq. (54), are:

i) additional degrees of freedom by the spin **S**, and

ii) coupling of **S** to the local AFM correlations.

To describe the local effects by this impurity center, we determine the m-nondiagonal GF's $\hat{G}_{\mathbf{k},\mathbf{k}'}$ from the equation of motion

$$\hat{G}_{\mathbf{k},\mathbf{k}'} = \frac{J}{N} \sum_{\mathbf{k}'',j} \alpha_{j,\mathbf{k}} \hat{G}_{\mathbf{k}} (s\hat{G}_{\mathbf{k}'',\mathbf{k}'} + \hat{G}^{(z)}_{\mathbf{k},\mathbf{k}'} + \hat{G}^{(-)}_{\mathbf{k},\mathbf{k}'}) \alpha_{j,\mathbf{k}''}$$

including three scattered GF's: the MF one $\hat{G}_{\mathbf{k}'',\mathbf{k}'}$, the longitudinal $\hat{G}^{(z)}_{\mathbf{k}'',\mathbf{k}'} = \langle\langle \psi_{\mathbf{k}''}(S_z - s) \,|\, \psi^{\dagger}_{\mathbf{k}'} \rangle\rangle$ and the transversal $\hat{G}^{(-)}_{\mathbf{k}'',\mathbf{k}'} = \langle\langle \overline{\psi}_{\mathbf{k}''} S_- \,|\, \psi^{\dagger}_{\mathbf{k}'} \rangle\rangle$ with the "spin-inverted" spinor $\overline{\psi}^{\dagger}_{\mathbf{k}} = (a^{\dagger}_{\mathbf{k},\downarrow}, a_{-\mathbf{k},\uparrow})$. The two last terms are analogous to the well known Nagaoka's Γ-term [73,74] and treating them with a similar decoupling procedure leads to the solution of type Eq. (50):

$$\hat{G}_{\mathbf{k},\mathbf{k}'} = \frac{1}{N} \sum_{j} \alpha_{j,\mathbf{k}} \hat{G}_{\mathbf{k}} \hat{T}_j \hat{G}_{\mathbf{k}'} \alpha_{j,\mathbf{k}'}, \tag{55}$$

but with more complicated partial T-matrices:

$$\hat{T}_j = [Js + J^2(\Sigma^2 \hat{G}_j + \hat{X}_j)][1 - Js - J^2(\Sigma^2 \hat{G}_j + \hat{X}_j)]^{-1},$$

where

$$\Sigma^2 = \langle S_z^2 \rangle - s^2, \quad \hat{X}_j = \frac{1}{N} \sum_{\mathbf{k}} \alpha^2_{j,\mathbf{k}} \hat{G}_{\mathbf{k}} (\varepsilon + h) \hat{X}_{\mathbf{k}},$$

$$\hat{X}_{\mathbf{k}} = S(S+1) - s(s+1) - \Sigma^2 + \left(1 + 2\frac{\xi_{\mathbf{k}}}{E_{\mathbf{k}}}\right)\hat{\tau}_3,$$

and the shift of energy argument, $\varepsilon \to \varepsilon + h$, is due to the nonelastic scattering effect of AFM stiffness.

It is interesting to trace the behavior of $\hat{T}_j$ in the two characteristic limits for AFM correlations between Cu^{2+} spins. In the paramagnetic limit: $h \to 0$, $s \to 0$, we have $\Sigma^2 \to S(S+1)/3$ and $\hat{X}_j \to 2S(S+1)/3$, so that

$$\hat{T}_j \to J^2 S(S+1) \hat{G}_j \left[1 - Js - J^2(\Sigma^2 \hat{G}_j + \hat{X}_j)\right]^{-1},$$

generalizing the known results [7,74] on the case of extended impurity center.

Another limit, fully polarized, $h \to \infty$, $s \to S$, corresponds to $\Sigma^2 \to 0$, $\hat{X}_j \to 0$ and results in

$$\hat{T}_j \to JS(1 - JS\hat{G}_j)^{-1}, \tag{56}$$

which is only due to MF magnetic scattering and similar to the simple forms, Eqs. (46), (47). This limit is justified at $JS \gg k_B T$, hence it well applies in the SC phase at $T < T_c \sim \Delta/k_B$ and will be used for the T-matrices below. The important change of the perturbation matrix structure, from $\hat{V} \propto \hat{\tau}_3$ to $\hat{V} \propto \hat{\tau}_0$, causes a strong modification of the impurity effects.

Thus, the variation of LDOS, Eq. (10), compared to the uniform value $\rho(\varepsilon)$, Eq. (9), is here presented as

$$\rho_{\mathbf{n}}(\varepsilon) - \rho(\varepsilon) = \frac{1}{\pi N} \mathrm{Im Tr} \sum_{\mathbf{k},\mathbf{k}' \neq \mathbf{k}} e^{i(\mathbf{k}-\mathbf{k}')\cdot\mathbf{n}} \hat{G}_{\mathbf{k},\mathbf{k}'} =$$

$$= \mathrm{Im Tr} \sum_{j} \hat{G}_j(\mathbf{n}) \hat{T}_j \hat{G}_j(\mathbf{n}),$$

where the matrices $\hat{G}_j(\mathbf{n}) = N^{-1} \sum_{\mathbf{k}} e^{i\mathbf{k}\cdot\mathbf{n}} \alpha^2_{j,\mathbf{k}} \hat{G}^{(0)}_{\mathbf{k}}$ appear by virtue of Eq. (55). The maximum LDOS variation is attained at $\mathbf{n} = \boldsymbol{\delta}$, the nearest neighbor sites to the impurity, mainly contributed by $j = 1$:

$$\rho_{\boldsymbol{\delta}}(\varepsilon) - \rho(\varepsilon) \approx \mathrm{Im Tr} \hat{G}_1(\boldsymbol{\delta}) \hat{T}_1 \hat{G}_1(\boldsymbol{\delta}). \tag{57}$$

The relevant GF matrices are obtained in similarity with Eq. (44):

$$\hat{G}_1(\boldsymbol{\delta}) \approx \overline{\alpha_1^2}\rho_N(g_0 + g_{\rm as}\hat{\tau}_3),$$

so that resulting $\rho_{\boldsymbol{\delta}}(\varepsilon)$ can display a resonance at $\varepsilon_{\rm res}$, defined by the denominator of $\hat{T}_1$:

$$\mathrm{Re}\,\{[1-u_A g_0(\varepsilon_{\rm res})]^2 - u_A^2 g_{\rm as}^2\} = 0, \qquad (58)$$

with the spin-dependent perturbation parameter $u_A = JS\rho_N\overline{\alpha_1^2}$, for the *A*-channel. Alike the case of nonmagnetic impurity, the finite asymmetry factor $g_{\rm as}$ makes it possible to have $\varepsilon_{\rm res}$ close to zero at rather moderate perturbation parameter J, close to $J_{\rm cr} = 1/(S\overline{\alpha_1^2}g_{\rm as}\rho_N)$, then the peak in LDOS becomes very sharp, as shown in Fig. 10 for $\rho_{\boldsymbol{\delta}}(\varepsilon)$ at the choice $J = 0.3$ eV $\approx 1.15 J_{\rm cr}$. The most notable distinction from the nonmagnetic perturbation consists in that the resonance condition $\mathrm{Re}\,g_0(\varepsilon_{\rm res}) = u_A^{-1} \pm g_{\rm as}$ for *odd* function $\mathrm{Re}\,g_0(\varepsilon)$ leads to a *single* sharp peak on one side from the Fermi level, instead of two symmetric peaks as in Figs. 3 and 6. This is just the observed behavior for LDOS near Zn sites in $Bi_2Sr_2CaCu_2O_8$ [18] (inset in Fig. 10), which is a strong argument in favor of the proposed perturbation mechanism for these impurities in CuO_2 planes.

The local effect on SC correlation is characterized by the same average $\Delta_{\mathbf{n}} = (V_{SC})\langle a_{\mathbf{n}+\boldsymbol{\delta}_1,\downarrow} a_{\mathbf{n}+\boldsymbol{\delta}_2,\uparrow}\rangle$ as in the preceding Section, and the suppression parameter $\eta_S = 1 - \Delta_0/\Delta$ is formally given by the same Eq. (52), but with the partial T-matrices defined by Eq. (56). Again, it is only contributed by the *E*-channel terms:

$$\eta_S = -\frac{2\int\limits_{-\infty}^{0} d\varepsilon\,\mathrm{Im}\mathrm{Tr}\hat{F}_2^0\hat{T}_2^0\hat{F}_2^0\hat{\tau}_1}{\int\limits_{-\infty}^{0} d\varepsilon\,\mathrm{Im}\mathrm{Tr}\hat{F}_{\boldsymbol{\delta}}^0\hat{\tau}_1} =$$

$$= -2u_E\int\limits_0^{\varepsilon_D} d\varepsilon\,\mathrm{Im}\,g_1\frac{2f_0 - u_E(2f_0g_0 + f_0^2 + g_1^2)}{D_E}\times$$

$$\times\left[\int\limits_0^{\varepsilon_D} d\varepsilon\,\mathrm{Im}\,g_1(\varepsilon)\right]^{-1}, \qquad (59)$$

where $D_E = (1-u_E g_0)^2 - u_E^2(g_1^2 + g_{\rm as}^2)$ and the spin-dependent perturbation parameter for *E*-channel $u_E = JS\rho_N\overline{\alpha_2^2}$. Comparing this function (see Fig. 11) to its analogue, Eq. (52), for the spin-independent perturbation, shows a much more pronounced suppression effect. The evident reason for this is the different structure of D_E in Eq. (59) compared to that in Eq. (47), directly related to the above mentioned change of the perturbation matrix structure.

In fact, numeric integration in Eq. (59) with the same set of parameters as used above for LDOS (corresponding to $u_E \approx 0.15$) shows a considerable suppression of local SC order: $\eta_S \approx 0.349$, almost triple of that for equal spin-independent perturbation in the previous Section. The dependence $\eta_S(J)$ is generally nonmonotonous, anyhow it should be stressed that no unitary limit $JS\rho_N \gg 1$ is needed to get such a strong effect.

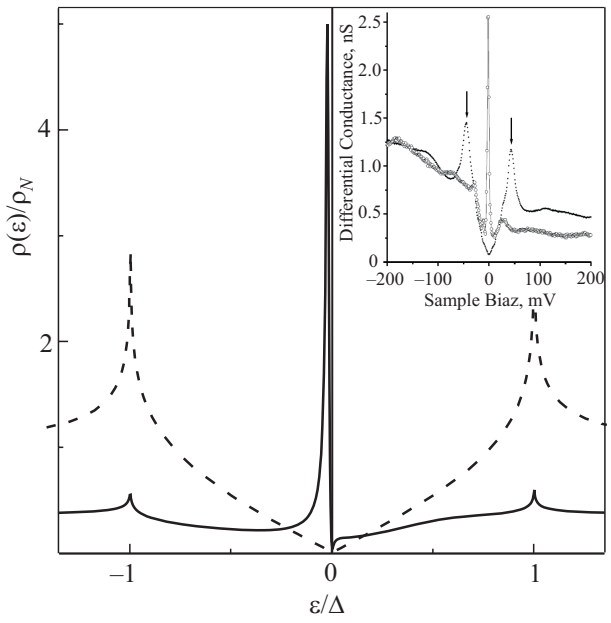

Fig. 10. Local density of states near magnetic impurity $\rho_{\boldsymbol{\delta}}(\varepsilon)$, given by Eqs. (57), (58), at the choice of perurbation parameter $J = 0.3$ eV, slighly above the critical value $J_{\rm cr} = 1/(S\overline{\alpha_1^2}g_{\rm as}\rho_N) \approx 0.26$ eV, presents a sharp resonance just below the Fermi level, similar to that observed in the STM spectrum on Zn site in $Bi_2Sr_2CaCu_2O_8$ at ≈ -1.5 meV [18] (inset).

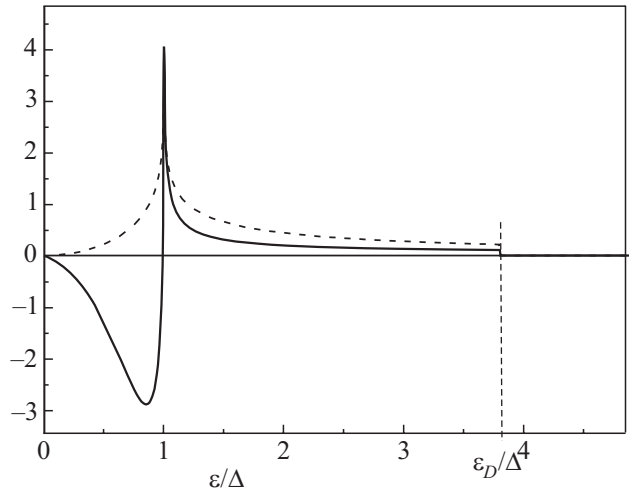

Fig. 11. The comparison between the behavior of dimensionless numerator (solid line) and denominator (dashed line) in Eq. (59).

6. Self-consistent approach and its validity

At higher concentrations of impurity scatterers the non-renormalized T-matrix approximation is no more reliable, and it is usually changed for its self-consistent version. In the simplest case of point-like scatterers, Eq. (3), we define the self-consistent approximation for m-diagonal GF as

$$\widehat{G}_{\mathbf{k}}^{(sc)} = \left\{ \left[\widehat{G}_{\mathbf{k}}^{(0)} \right]^{-1} - \hat{\Sigma}^{(sc)} \right\}^{-1}, \qquad (60)$$

including the self-consistent matrices for self-energy:

$$\hat{\Sigma}^{(sc)} = -c\hat{V}\left[1 + \widehat{G}^{(sc)}\hat{V} \right]^{-1} \qquad (61)$$

and for local GF:

$$\widehat{G}^{(sc)} = \frac{1}{N}\sum_{\mathbf{k}} \widehat{G}_{\mathbf{k}}^{(sc)}. \qquad (62)$$

The self-energy matrix, Eq. (61), is expanded in Pauli matrices:

$$\hat{\Sigma}^{(sc)} = \Sigma_0 + \Sigma_1\hat{\tau}_1 + \Sigma_3\hat{\tau}_3, \qquad (63)$$

where Σ_i are generally some complex-valued functions of energy [55]. Then integration in Eq. (62), using Eq. (11), results in a similar expansion for the self-consistent GF matrix:

$$\widehat{G}^{(sc)} = G_0 - G_1\hat{\tau}_1 - G_3\hat{\tau}_3. \qquad (64)$$

It can be easily shown that the self-consistent value of $G_1(\varepsilon)$ is actually zero [55], and G_3 is practially constant: $G_3 \approx \rho_N g_{\mathrm{as}}$, hence the self-consistency problem for point-like impurities in the *d*-wave SC is reduced to that for the complex function $G_0(\varepsilon) = \rho_N g_0(\varepsilon - \Sigma_0)$ defined by the equation for scalar self-energy $\Sigma_0(\varepsilon)$:

$$1 - v^2 g_0(\varepsilon - \Sigma_0)\left[g_0(\varepsilon - \Sigma_0) - \frac{c}{\Sigma_0\rho_N} \right] = 0. \qquad (65)$$

In the most important region of low energies, $|\varepsilon| \ll \Delta$, this equation can be simplified, presenting g_0 in the logarithmic approximation:

$$g_0(\varepsilon) \approx \frac{\varepsilon}{\Delta}\left(\ln\frac{|\varepsilon|}{4\Delta} + i\frac{\pi}{2} \right) + \frac{\varepsilon}{4\pi\tilde{\mu}}, \qquad (66)$$

instead of exact elliptic functions, Eq. (13). Considering Eq. (65), P. Lee supposed that in the *unitary* limit, $v \to \infty$, the unity term can be dropped [36], then the self-energy gets related to the local GF as $\Sigma_0 = -c/G_0$ (inverse to the common relation $\Sigma_0 \approx cv^2 G_0/\rho_N^2$ in the Born limit, $v \ll 1$). This surprising relation leads directly to the conclusion that, in a *d*-wave superconductor with unitary scatterers, the self-energy should tend to a *finite* limiting value: $\Sigma_0(\varepsilon \to 0) \to -i\gamma_0$, and so the DOS: $\rho(\varepsilon \to 0) \to \rho_0 = c/(\pi\gamma_0)$, or in the present notations: $\rho_0 \approx \sqrt{\pi c\rho_N/\Delta}$ (within to some logarithmic corrections and neglecting the terms $\sim \Delta/\tilde{\mu}$ beside unity). A similar conclusion for the case of Born scatterers, $v \ll 1$, was made earlier by Gor'kov and Kalugin [75], and their predicted finite DOS reads in these notations as $\rho_0 \approx (4\pi\rho_N/\alpha)\mathrm{e}^{-1/\alpha}$ with $\alpha = \pi c v^2/(\rho_N\Delta) \ll 1$.

These finite limits should mean a spontaneous breakdown of the *d*-wave symmetry in presence of scatterers and a qualitative rearrangement of the low-energy excitation spectrum, including appearance of strongly localized quasiparticle states (in spite of absence of such localization in the simple T-matrix treatment [14,15]). The last decade produced an extensive theoretical discussion on reality of such SCTMA behavior, and an astonishing variety of results was obtained, including a power law convergence to zero: $\rho(\varepsilon \to 0) \propto \varepsilon^{\alpha}$, with universal [76] or nonuniversal [51,77] values of the exponent α, different finite limits $\rho(\varepsilon \to 0) \to \rho_0$ [36,75,78] and even a divergence $\rho(\varepsilon \to 0) \propto \varepsilon\ln(1/\varepsilon)$ [79]. On the other hand, numerous experimental studies have been done to check the principal conclusion from the existence of finite ρ_0 in the unitary limit, the so-called *universal* values of quasiparticle electrical conductivity $\sigma_0 = (e^2/\pi^2\hbar)v_F/v_\Delta$ [36] and heat conductivity $\kappa_0/T = (k_B^2/3)(v_F^2 + v_\Delta^2)/v_F v_\Delta$ [38], and also the results of these measurements are still contradictory.

It should be stressed that the above mentioned theoretical construction uses the two main assumptions: i) that certain impurities in high-T_c superconductors are extremely strong scatterers (even as high values as $v \sim 10^2$–10^3 are used sometimes to adjust the theoretical predictions to observable data); ii) that solutions of self-consistent equations (linear in c) can apply either to extended and localized states (since the finite ρ_0 relates to localized states).

However, even for possibly high value of v (enhanced by the above discussed asymmetry factor, though less probable to exceed few units), the neglect of the unity term in Eq. (65) may be unjustified at very low energies. This rises a technical question about existence of different formal solutions of this equation. But a more fundamental issue is that the self-consistency procedure is only well defined for *extended* electronic states [80], which assure effective averaging of effects of random impurity scatterers, say, along the mean free path. This suggests to additionally check whether the obtained solutions are compatible with the self-consistency, and, if they do not, to look for alternative solutions, beyond the framework of SCTMA. Below we consider in more detail whether the finite DOS at zero energy necessarily follows from the SCTMA solution and which alternatives can exist for it [81].

Equation (65) can be formally solved with respect to $g_0(\varepsilon - \Sigma_0)$:

$$g_0(\varepsilon - \Sigma_0) = \frac{-c \pm \sqrt{c^2 + (2\Sigma_0\rho_N/v)^2}}{2\Sigma_0\rho_N}, \qquad (67)$$

so that the Lee's choice in the unitary limit (at $|v| \gg 2\rho_N |\Sigma_0|/c$) is related to the *minus* sign while the Gor'kov and Kalugin's choice in the Born limit (at $|v| \ll 2\rho_N |\Sigma_0|/c$) to the *plus* sign. Also we notice that, taking into account the functional forms as Eqs. (13) or (66) for $g_0(\varepsilon - \Sigma_0)$, the l.h.s. of Eq. (65) defines a rather complicated expression for Σ_0 in function of energy ε and, for arbitrary perturbation parameter v, it generally displays multiple roots. Then a single physical solution for any given energy ε should be selected on the basis of SCTMA validity criterion (this analysis will be done in the next Section).

The numerical solutions of Eq. (65) in the complex plane of self-energy Σ_0 for different values of ε and v are summarized in Fig. 12. It is seen that there are two roots in each case, denoted SCTMA_1 and SCTMA_2. The SCTMA_2 root tends to a finite and imaginary value at $\varepsilon \to 0$, and, passing to the unitary or Born limits in v, one reproduces respectively the Lee's and Gor'kov and Kalugin's predictions in a unified way. At the same time, the SCTMA_1 root tends to zero at $\varepsilon \to 0$ for *any* value of v, suggesting a zero limit for the DOS. This general behavior is essentially the same for both functional forms of g_0 in Eq. (65). Hence, at any regime of impurity perturbation, there is an alternative to the finite limit of low-energy DOS, consistently calculated within the SCTMA framework!

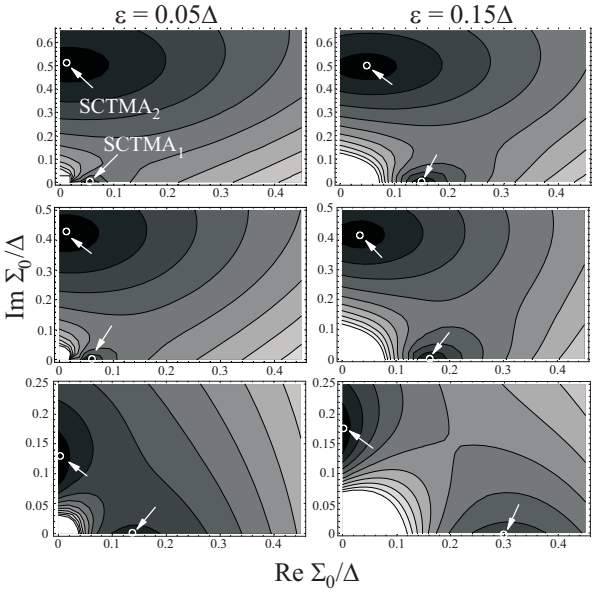

Fig. 12. Contour plots of the left hand side of Eq. (65), in function of complex self-energy Σ_0 for two different energies ε at the choice of $c = \rho_N \Delta$ and three different perturbation parameters: unitary limit $v = 10$ (upper row), intermediate regime $v = 1$ (middle row), and Born limit $v = 0.35$ (bottom row). There are always two roots shown by white circles and denoted SCTMA_1 and SCTMA_2, and at $\varepsilon \to 0$ the first of them tends to zero, close to the real axis, while the other tends to a finite imaginary limit.

One additional comment is in order to the self-consistent equation with multiple solutions, like that in Fig. 12. It is seen there that the SCTMA_2 root have a much wider "attraction basin" than SCTMA_1, especially at very low energies. This can hinder detection of the alternative solution when running a numeric routine, as probably was the case for several numerical SCTMA studies which found finite DOS at zero energy [51,78].

It will be seen below that each of the two suggested SCTMA solutions has its specific validity domain, beyond the area of impurity resonance, while no one of them is a good approximation within this area. Let us specify the low-energy behavior of each solution and try to build a "pragmatic" combination of the two, in order to obtain a correctly normalized quasiparticle DOS.

The low-energy limit for the SCTMA_2 solution, $\Sigma_0(\varepsilon \to 0) = -i\gamma_0$, is obtained accordingly to Eq. (65) as a root of

$$1 + v^2 \left[2\mathrm{K}\left(-\frac{\Delta^2}{\gamma_0^2} \right) + \frac{\gamma_0}{2\tilde{\mu}} \right]^2 + \frac{cv^2}{\rho_N \gamma_0} \left[2\mathrm{K}\left(-\frac{\Delta^2}{\alpha_0^2} \right) + \frac{\gamma_0}{2\tilde{\mu}} \right] = 0, \tag{68}$$

in the "elliptic" form, or

$$1 + v^2 \gamma_0^2 \left(\frac{2}{\Delta} \ln \frac{4\Delta}{\gamma_0} - \frac{1}{\tilde{\mu}} \right)^2 - \frac{cv^2}{\rho_N} \left(\frac{2}{\Delta} \ln \frac{4\Delta}{\gamma_0} - \frac{1}{\tilde{\mu}} \right) = 0, \tag{69}$$

in the "logarithmic" form. The numeric solution of Eq. (69) for γ_0 in function of perturbation parameter v (shown in Fig. 13 for the choice of $c = \rho_N \Delta$) reproduces the Lee's limit already for $v \gtrsim 3$ and the Gor'kov and Kalugin's limit for $v \lesssim 0.5$ and thus justifies the attribution of regimes in Fig. 12. The result for Eq. (68) is essentially the same.

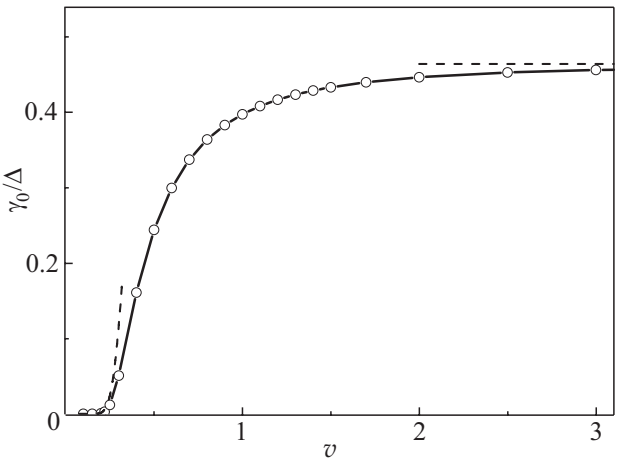

Fig. 13. Residual self-energy $\gamma_0 = \lim_{\varepsilon \to 0} i\Sigma(\varepsilon)$ for the SCTMA_2 solution, calculated from Eq. (69) with the choice of $\tilde{\mu} = 10\Delta$ in function of the perturbation parameter v (open circles). The dashed lines show the limiting behaviors: exponential in the Born limit, $\gamma_0/\Delta \approx 4\exp(-\rho_N \Delta/\pi c v^2)$, and a constant value in the unitary limit.

The behavior of the SCTMA$_2$ solution at finite energies ε can be obtained from Eq. (65) only numerically, and the related DOS, as shown in Fig. 14, grows slowly from the residual value ρ_0 at $\varepsilon \lesssim \varepsilon_{\rm res}$ and then at $\varepsilon > \varepsilon_{\rm res}$ goes closely to the result of simple T-matrix approximation of Sec. 4, which suggests reliability of SCTMA$_2$ in this energy range.

For the alternative SCTMA$_1$ solution, Eq. (65) admits an analytical approximation* by using the logarithmic asymptotics for the elliptic K-integral (or $\arcsin x \approx \approx -i\ln(2ix)$ at $|x| \gg 1$ [55] for the arcsine form):

$$G_0(\varepsilon) \approx \frac{\rho_N^2 \varepsilon}{cv^2 \ln\left(4icv^2/\rho_N\varepsilon\right)}. \tag{70}$$

The corresponding analytic function for the low-energy DOS is

$$\rho(\varepsilon) \approx \frac{\rho_N^2 \varepsilon}{cv^2 \ln^2\left(4cv^2/\rho_N\varepsilon\right)}, \tag{71}$$

though, for the instance in Fig. 14, the numerical SCTMA$_1$ solution attains this behavior only at $\varepsilon \lesssim 10^{-3}\Delta$. However, it is just this function that describes the asymptotic vanishing of DOS, even faster than the nonperturbed function, Eq. (14) or the simple T-matrix function, Fig. 3. Also it vanishes faster than the power laws, $\rho(\varepsilon) \propto \varepsilon^{\alpha}$ with

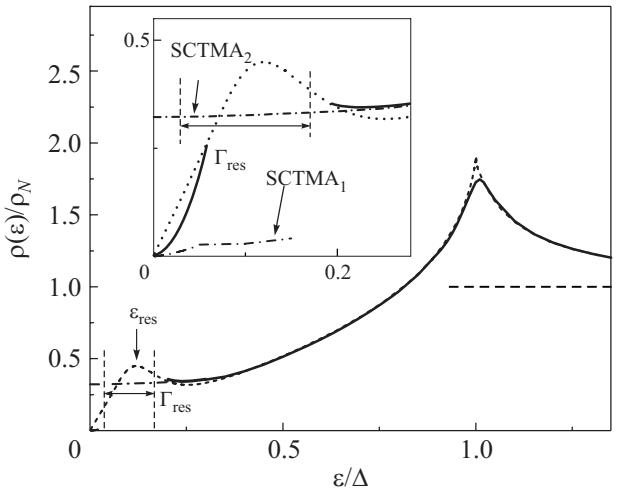

Fig. 14. Construction of the self-consistent DOS (solid line) adjusted to the two different SCTMA solutions beyond the region of impurity resonance $\varepsilon_{\rm res}$ of width $\Gamma_{\rm res}$. The impurity parameters are chosen as $v = 1$ and $c = 0.2\rho_N\Delta$. The SCTMA$_1$ solution is shown by the dashed line, the SCTMA$_2$ solution by the dash-dotted line, and the short-dash line shows the common T-matrix solution from Fig. 3.

$\alpha \le 1$ [51,77], or with $\alpha = 1$ [76], using other than SCTMA approaches. That fast vanishing can be seen as a certain narrow "quasi-gap" near the Fermi energy, and beyond this quasi-gap a plausible matching between the two SCTMA solutions, over the interval of broadening $\Gamma_{\rm res}$ of the resonance $\varepsilon_{\rm res}$, can be done by the simple T-matrix function, in order to preserve the overall normalization of DOS [68]

$$\int d\varepsilon\left[\rho(\varepsilon) - \rho_N\right] = 0. \tag{72}$$

Notice that Eq. (72) is already satisfied if $\rho(\varepsilon)$ is chosen in the simple T-matrix form (short-dash line in Fig. 14). Hence it is also satisfied if the positive and negative areas between that and SCTMA (solid line) curves in the energy intervals beyond the $\Gamma_{\rm res}$ range are equal, as approximately realized by the construction in Fig. 14. This provides the sought "compromise" SCTMA solution for DOS.

6.1. Ioffe–Regel–Mott criterion and validity of SCTMA solutions

A criterion for a quasiparticle state with excitation energy ε and momentum p to be of extended type, as necessary for the SCTMA solutions, was first proposed by Ioffe and Regel [82] and then substantiated by Mott [27], consisting in that the quasiparticle mean free path ℓ be longer than its wavelength $\lambda = 2\pi\hbar/p$, or else that its lifetime τ be longer than the oscillation period $\hbar/\varepsilon$. This criterion is widely used for analysis of normal excitation spectra in disordered systems [80], however, when applying it to disordered superconductors, one has first to redefine the quasiparticle basic characteristics. Thus, excitation of a Bogolyubov quasiparticle with the nominal wave vector $\mathbf{k}$ over the BCS ground state changes the system energy by $E_{\mathbf{k}}$ and hence its momentum by $p_{\mathbf{k}} = \hbar E_{\mathbf{k}} / \left|\nabla_{\mathbf{k}} E_{\mathbf{k}}\right|$. Then the related wavelength is $\lambda_{\mathbf{k}} = 2\pi\left|\nabla_{\mathbf{k}} E_{\mathbf{k}}\right| / E_{\mathbf{k}}$, generally different from the free particle value $2\pi/k$. Next, the mean free path $\ell_{\mathbf{k}}$ is defined as the group velocity $\left|\nabla_{\mathbf{k}} E_{\mathbf{k}}\right|/\hbar$ times the lifetime $\hbar/\mathrm{Im}\Sigma(E_{\mathbf{k}})$, so that the Ioffe–Regel–Mott (IRM) criterion $\ell_{\mathbf{k}} \gg \lambda_{\mathbf{k}}$ can be presented as

$$E_{\mathbf{k}} \gg \mathrm{Im}\Sigma\left(E_{\mathbf{k}}\right). \tag{73}$$

In fact, the dispersion law is renormalized due to impurity scattering, passing from $E_{\mathbf{k}} = \sqrt{\xi_{\mathbf{k}}^2 + \Delta_{\mathbf{k}}^2}$ to $\widetilde{E}_{\mathbf{k}}$ defined by

$$\widetilde{E}_{\mathbf{k}} - \mathrm{Re}\Sigma(\widetilde{E}_{\mathbf{k}}) = E_{\mathbf{k}}. \tag{74}$$

Using the simple T-matrix solution, $\Sigma = cv^2\rho_N^{-1} g_0 / (1 - v^2 g_0^2)$, we have in the long-wave limit:

* But only valid at extremely low energies.

$$\widetilde{E}_{\mathbf{k}} \approx \frac{\rho_N \Delta}{cv^2 \ln(4cv^2/\rho_N E_{\mathbf{k}})} E_{\mathbf{k}},$$

$$\mathrm{Im}(\widetilde{E}_{\mathbf{k}}) \approx \frac{cv^2}{\rho_N \Delta} \widetilde{E}_{\mathbf{k}} \approx \frac{E_{\mathbf{k}}}{\ln(4cv^2/\rho_N E_{\mathbf{k}})}. \qquad (75)$$

Thus the criterion (73) is only fulfilled for low enough concentration of scatterers:

$$c < c_\Delta \equiv \rho_N \Delta / v^2,$$

and this can be considered the validity condition for simple T-matrix approximation.

At higher impurity concentrations, $c \gg c_\Delta$, we need to pass to the SCTMA solutions of the preceding Section and to renormalize the dispersion law $\widetilde{E}_{\mathbf{k}}$ and self-energy $\Sigma(\widetilde{E}_{\mathbf{k}})$ in a way specific for each solution [83]. Since the SCTMA self-energy only depends on energy, not on momentum, Eq. (74) holds for any relation between the radial and tangential components, $\xi_{\mathbf{k}}$ and $\Delta_{\mathbf{k}}$, of excitation energy $E_{\mathbf{k}}$. In particular limits: i) $\Delta_{\mathbf{k}} \to 0$, $E_{\mathbf{k}} \to \xi_{\mathbf{k}}$ and ii) $\xi_{\mathbf{k}} \to 0$, $E_{\mathbf{k}} \to \Delta_{\mathbf{k}}$, the limiting values are renormalized accordingly to the equations

$$\text{i)} \quad \tilde{\xi}_{\mathbf{k}} - \mathrm{Re}\Sigma(\tilde{\xi}_{\mathbf{k}}) = \xi_{\mathbf{k}},$$

$$\text{ii)} \quad \tilde{\Delta}_{\mathbf{k}} - \mathrm{Re}\Sigma(\tilde{\Delta}_{\mathbf{k}}) = \Delta_{\mathbf{k}}.$$

Then, using the SCTMA$_1$ solution (in elliptic K-form) in Eq. (74), we estimate the long-wave dispersion law within logarithmic accuracy as

$$\widetilde{E}^{(1)}_{\mathbf{k}} \approx \frac{c}{c_\Delta} E_{\mathbf{k}} \ln \frac{4\Delta}{E_{\mathbf{k}}}$$

(note the difference from Eq. (75) for simple T-matrix). Respectively, its limiting values are renormalized as

$$\tilde{\xi}^{(1)}_{\mathbf{k}} \approx \frac{c}{c_\Delta} \xi_{\mathbf{k}} \ln \frac{4\Delta}{E_{\mathbf{k}}}, \quad \tilde{\Delta}^{(1)}_{\mathbf{k}} \approx \frac{c}{c_\Delta} \Delta_{\mathbf{k}} \ln \frac{4\Delta}{E_{\mathbf{k}}},$$

and the related damping:

$$\Gamma^{(1)}_{\mathbf{k}} = \mathrm{Im}\Sigma^{(1)}(\widetilde{E}^{(1)}_{\mathbf{k}}) \approx \frac{\pi E_{\mathbf{k}}}{2\ln(4\Delta/E_{\mathbf{k}})}.$$

Using this in the IRM criterion, Eq. (73), leads to the SCTMA$_1$ validity condition:

$$E_{\mathbf{k}} \ll \Delta \exp\left(-\sqrt{\frac{\pi c_\Delta}{2c}}\right), \qquad (76)$$

which holds in a very narrow vicinity of the Fermi energy at $c < c_\Delta$. At $c > c_\Delta$, the corresponding validity condition is already obtained from the nonrenormalized dispersion law: $E_{\mathbf{k}} \gg \Gamma^{(1)}_{\mathbf{k}}$, and this defines a broader vicinity of Fermi level $E_{\mathbf{k}} \ll \Delta$ (its numerical smallness can be, for instance, as $\sim 10^{-2}\Delta$). The above discussed relations between real and imaginary parts of the two solutions for self-energies $\Sigma^{(1),(2)}$ are illustrated in Fig. 15.

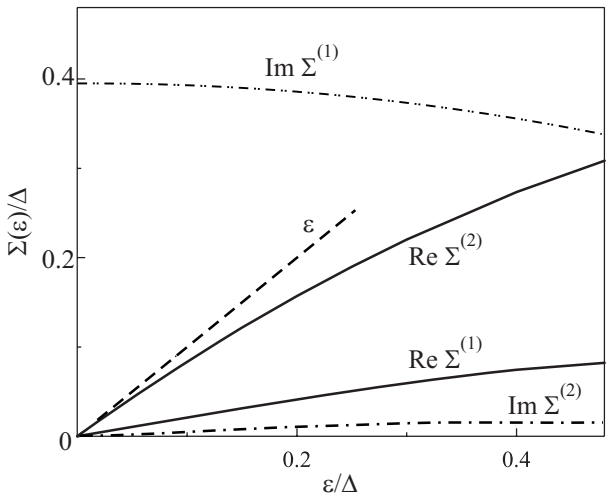

Fig. 15. Real and imaginary parts of the self-energy $\Sigma(\varepsilon)$ (in units of Δ) obtained for two different SCTMA solutions at the choice of perturbation parameters $c = \rho_N \Delta$, $v = 1$. Note the tendency of $\mathrm{Re}\Sigma^{(2)}(\varepsilon)$ to ε (dashed line) at $\varepsilon \to 0$.

Applying the same treatment to the SCTMA$_2$ solution, which formally defines the low-energy dispersion law $\widetilde{E}^{(2)}_{\mathbf{k}} \approx E_{\mathbf{k}}$ and the damping $\Gamma^{(2)}_{\mathbf{k}} = \mathrm{Im}\Sigma^{(2)}(\widetilde{E}^{(2)}_{\mathbf{k}}) \approx \approx cv^2 \rho_N^{-1} \mathrm{Im} g_0$, we obtain the condition

$$E_{\mathbf{k}} \gg \frac{c}{c_\Delta} \Delta \, \mathrm{Im}\, g_0(E_{\mathbf{k}}), \qquad (77)$$

so that this solution is valid only far enough from the nodal points, where it provides the correct limit of pure *d*-wave DOS. However, this solution is clearly eliminated near the nodal point. Thus, the only SCTMA solution, which may be valid in a close vicinity of the Fermi energy, is the SCTMA$_1$ solution, Eq. (71).

Notably, the two estimates, Eqs. (76), (77), do not necessarily assure the overlap between the two validity regions, so that for $c \gg c_\Delta$ there can exist some intermediate energy range where neither of SCTMA solutions applies. This range roughly corresponds to the broad linewidth of the impurity resonance $\varepsilon_{\mathrm{res}}$ where DOS cannot be rigorously obtained even with use of the next GE terms, and where it was interpolated by the simple T-matrix form between the two SCTMA asymptotics in the previous Section.

Finally, we notice that other known nonperturbative solutions for *d*-wave disordered systems with DOS vanishing at $\varepsilon \to 0$ as a certain power law: $\rho(\varepsilon) \sim \varepsilon^\alpha$ [76,77], also have to obey the IRM criterion since they use the field theoretic approach, only compatible with band-like states. But it can be easily shown that the IRM criterion is only fulfilled for such DOS if the power is $\alpha > 1$, while the reported values are $\alpha = 1/7$ [77] and $\alpha = 1$ [76]. In fact, let the renormalized components of dispersion law (in the low-energy limit) depend on the

effective nodal variables ξ and η by power laws, $\tilde{\xi}_k \propto \xi^{\nu}$ and $\tilde{\Delta}_k \propto \eta^{\nu}$, with a certain $\nu > 0$. Then the simplest estimate for the *d*-wave DOS is

$$\rho(\varepsilon) \propto \varepsilon \int d\Delta \int d\xi\, \delta(\varepsilon^2 - \tilde{\xi}^2 - \tilde{\Delta}^2) \propto \varepsilon \int E\delta(\varepsilon^2 - \tilde{E}^2)\, dE =$$

$$= \varepsilon \int E\delta(\varepsilon^2 - E^{2\nu})\, dE \propto \varepsilon^{2/\nu - 1},$$

that is the DOS exponent $\alpha = 2/\nu - 1$. In the considered field models, the quasiparticle broadening is expressed through the DOS: $\Gamma_{\mathbf{k}} = u^2 \rho(\tilde{E}_b k)$, with the disorder parameter u of the Anderson model [28]. Then the criterion, Eq. (73), is reformulated as

$$\tilde{E} \gg u^2 \rho(\tilde{E}),$$

and leads to the condition $\tilde{E} \gg \text{const} \cdot \tilde{E}^{2/\nu - 1}$. In the limit $\tilde{E} \to 0$, this is only possible if $2/\nu - 1 > 1$, that is $\alpha > 1$.

7. Group expansions and localization of nodal quasiparticles

The above considerations essentially restrict possible candidate solutions for quasiparticle spectrum in the disordered *d*-wave superconductor and may suggest Eq. (71) as the only consistent low-energy solution for the problem.

However the SCTMA (or field-theoretical) analysis can not be considered fully comprehensive for the real quasiparticle spectrum in a disordered system, if the localized states are also admitted. In accordance with the above IRM check, the single-impurity scattering processes by SCTMA can not produce localized states near zero energy. But if the SCTMA contribution to DOS vanishes in this limit, the importance can pass to the next GE terms, related to scattering (and possible localization) of quasiparticles on random groups (clusters) of impurities. The essential point is that their contribution to DOS is mostly defined by the *real* parts of GF's which do not need self-consistency corrections and thus remain valid for the energy range of localized states (where the IRM criterion no more holds).

The known approaches to impurity cluster effects in disordered *d*-wave superconductors, either numerical [56,84] and analytical [79], were contradictory about the DOS behavior and did not conclude definitely on localization. A practical analysis of such effects within the GE framework, using a special algebraic technique, was proposed for an *s*-wave superconductor in the limit $\varepsilon \to \Delta$ [85]. A similar technique for disordered *d*-wave systems in the limit $\varepsilon \to 0$ is presented below for the cases of nonmagnetic (NM) and magnetic (M) impurities, showing that only M impurities can provide a finite DOS in this limit, replacing the SCTMA_1 solution (and different from the SCTMA_2) in a narrow vicinity of the nodal energy, manifesting the onset of localization there. In particular, this should produce, instead of universal conductivity, its exponential suppression at sufficiently low temperatures.

7.1. Interaction matrices and DOS at nodal points

We pass to consideration of the states near the Fermi level, $\varepsilon \to 0$, with use of the nonrenormalized GE, Eq. (28) (expected to be more adequate for localized states). Then the limit value for DOS $\rho(\varepsilon \to 0)$ is related with the imaginary and traceful part of the self-energy matrix: $\sigma = \text{Tr}\,\text{Im}\hat{\Sigma}_{\mathbf{k}}(0)/2$ (for simplicity, we drop the super-indices at all nonrenormalized GE matrices). If the main contribution to γ comes from the GE pair term, Eq. (30), where the share of $\hat{A}_{\mathbf{n}} e^{-i\mathbf{k}\cdot\mathbf{n}}$ is negligible beside that of $\hat{A}_{\mathbf{n}}\hat{A}_{-\mathbf{n}}$, the value of γ can be considered momentum-independent. In this approximation, supposing also $\gamma \ll \Delta$, one obtains [36]

$$\rho(0) \approx \rho_N \frac{2\sigma}{\pi\Delta} \ln\frac{\Delta}{\sigma}, \tag{78}$$

and the following task is reduced to the proper calculation of σ in function of the impurity perturbation parameters. Then we present the interaction matrices at $\varepsilon \ll \Delta$ as

$$\hat{A}_{\mathbf{n}}(\varepsilon) = \left[g_0(\mathbf{n}) + g_3(\mathbf{n})\hat{\tau}_3 + g_1(\mathbf{n})\hat{\tau}_1\right]\hat{T}(0), \tag{79}$$

where the coefficient functions

$$g_0(\mathbf{n}) = \frac{\varepsilon}{N}\sum_{\mathbf{k}} \frac{e^{i\mathbf{k}\cdot\mathbf{n}}}{\varepsilon^2 - E_{\mathbf{k}}^2},$$

$$g_3(\mathbf{n}) = \frac{1}{N}\sum_{\mathbf{k}} \frac{e^{i\mathbf{k}\cdot\mathbf{n}}\xi_{\mathbf{k}}}{\varepsilon^2 - E_{\mathbf{k}}^2},$$

$$g_1(\mathbf{n}) = \frac{1}{N}\sum_{\mathbf{k}} \frac{e^{i\mathbf{k}\cdot\mathbf{n}}\Delta_{\mathbf{k}}}{\varepsilon^2 - E_{\mathbf{k}}^2} \tag{80}$$

are obtained using the linearized dispersion laws near the nodal points $\mathbf{k}_{j=1,\ldots,4}$ (see Fig. 16): $\xi_{\mathbf{k}} \approx \hbar v_F q_1$, $\Delta_{\mathbf{k}} \approx \hbar v_\Delta k_2$, where the 1- and 2-components are along the diagonals of the Cartesian basis and the characteristic

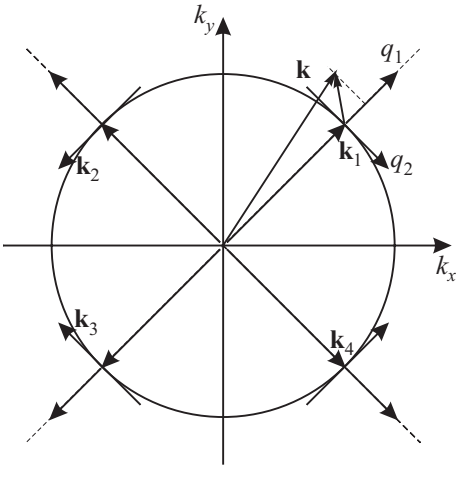

Fig. 16. Schematic of local coordinates near nodal points in the Brillouin zone of a *d*-wave superconductor.

velocities v_F and v_Δ are related as $v_\Delta / v_F = \beta = \Delta / \mu \ll 1$. Then, after summing over nodal points, the above functions are expressed as

$$g_l(\mathbf{n}) = f_l(n_1, n_2)\cos k_F n_1 + f_l(n_2, n_1)\cos k_F n_2, \qquad (81)$$

that is superpositions of fast oscillating Fermi cosines with slowly decaying amplitudes. The first such amplitude reads

$$f_0(n_1, n_2) = \frac{\rho_N \varepsilon}{4\Delta} \int_{-\mu}^{W-\mu} d\xi \int_{-\Delta}^{\Delta} d\eta \times$$

$$\times \frac{\exp\left[i\left(\xi n_1 / \hbar v_F + \eta n_2 / \hbar v_\Delta\right)\right]}{\varepsilon^2 - \xi^2 - \eta^2}, \qquad (82)$$

and its reasonable approximation for low energies, $|\varepsilon| \ll \Delta$, and long enough distances, $k_F |n_{1,2}| \gg 1$, is given by the extension of integration to infinite limits:

$$f_0(n_1, n_2) \approx -i \frac{\pi \rho_N \varepsilon}{2\Delta} H_0^{(1)}\left(\sqrt{n_1^2 / \ell_F^2 + n_2^2 / \ell_\Delta^2}\right). \qquad (83)$$

Here $H_0^{(1)}$ is the Hankel function of the first kind [49] and $\ell_i = \hbar v_i / \varepsilon$ are its radial and tangential decay lengths (notice their divergence at $\varepsilon \to 0$). The logarithmic divergence of the formula, Eq. (83), at formal limit $k_F |n_{1,2}| \to 0$, is restricted to the level of $g_0(\varepsilon) \sim \rho_N \varepsilon \ln(\Delta / \varepsilon)$, that is corresponding to $k_F |n_{1,2}| \sim 1$. The corrections due to the finite integration limits have much shorter decay lengths (not longer than the SC coherence length) and thus can be safely neglected. Other amplitudes in Eq. (81) are expressed through the above one

$$f_3(n_1, n_2) = -i\ell_F \frac{\partial f_0(n_1, n_2)}{\partial n_1},$$

$$f_1(n_1, n_2) = -i\ell_\Delta \frac{\partial f_0(n_1, n_2)}{\partial n_2}. \qquad (84)$$

In the limit $\varepsilon = 0$, the matrices $\hat{T}(0)$ and $\hat{A}_\mathbf{n}$ are purely real (see the next Section), then the imaginary part of the GE pair term is generated by the poles of the inverse matrix $(1 - \hat{A}_\mathbf{n} \hat{A}_{-\mathbf{n}})^{-1}$. Here we notice that, from Eqs. (83), (84), the interaction matrix in the limit $\varepsilon = 0$ is "odd" in its vector argument: $\hat{A}_{-\mathbf{n}} = -\hat{A}_\mathbf{n}$. If there is no such poles, one has to search for contributions to γ from the next order GE terms. Thus, for an lth order GE term, the imaginary part is related to the poles of the inverse of a certain lth degree polynomial in $\hat{A}_{\mathbf{n}_1}, \ldots, \hat{A}_{\mathbf{n}_{l(l-1)/2}}$ (where $\mathbf{n}_1, \ldots, \mathbf{n}_{l(l-1)/2}$ are all possible separations between l impurities).

Generally, in the energy spectrum of a crystal with impurities, one can distinguish certain intervals where DOS is dominated by different types of states: i) band-like states, ii) localized states by single impurities, iii) those by close impurity pairs (that is closer than the average separation $\sim a/\sqrt{c}$ between impurities), iv) by close triples, etc. [26]. Then, e.g., in the pair-dominated energy interval, each discrete peak is due to all impurity pairs with a given close separation n, and it experiences small shifts, due to farther impurity neighbors of each pair, different in different parts of the system. These shifts produce broadening of pair peaks, and if this broadening is wider than the distance between the peaks, the resulting continuous spectrum of pair-dominated type can be effectively described by passing from summation in discrete $\mathbf{n} \neq 0$ in Eqs. (26), (30) to integration in continuous $\mathbf{r}$ (for $r \gg a$). Such possibility was shown long ago for normal electron spectrum [43], but a specifics for a superconducting system with disorder is in the aforementioned oscillating interaction between impurities and the related multiplicity of pole contributions to DOS. The detailed analysis of matrix GE terms is also specified by the particular matrix forms for impurity perturbation, as shown below.

7.2. Nonmagnetic impurities

The expansion, Eq. (79), of interaction matrices $\hat{A}_\mathbf{n}$ in the set of $\hat{\tau}_l$ with oscillating and complex coefficient functions, makes it quite a hard problem to calculate even the pair GE term, to say nothing about higher order terms. However this problem can be essentially simplified in the limit $\varepsilon = 0$, when the function g_0 identically vanishes and $g_{1,3}$ are finite and real. In a similar situation for matrix GE in *s*-wave superconductors, the algebraic isomorphism between the interaction Nambu matrices and common complex numbers was used [85], permitting to reduce the matrix problem to much easier complex analysis. Remarkably, the same isomorphism is also found for the case of NM impurities in the *d*-wave system at zero energy [86]. Here we have explicitly: $\hat{T}(0) = \tilde{V}\hat{\tau}_3$, where $\tilde{V} = v/\rho_N$, and the interaction matrices, Eq. (79), are presented as $\hat{A}_\mathbf{n} = \tilde{V} g_3(\mathbf{n}) + i\tilde{V} g_1(\mathbf{n})\hat{\tau}_2$, thus pertaining to the general two-parametric family $\hat{C}(x, y) = x + iy\hat{\tau}_2$ with real x, y. This family forms an algebra with the product $\hat{C}(x, y)\hat{C}(x', y') = \hat{C}(xx' - yy', yx' + xy')$, isomorphic to that considered in Ref. 85 and to the algebra $\mathbb{C}$ of common complex numbers: $(x + iy)(x' + iy') = xx' - yy' + i(yx' + xy')$. By this isomorphism, the real matrix $\hat{A}_\mathbf{n}$ is seen as a "complex number" $A_\mathbf{n} = \tilde{V} g_3(\mathbf{n}) + \hat{i}\tilde{V} g_1(\mathbf{n})$, where the "imaginary unity" $\hat{i}$ corresponds to the *real* matrix $\hat{i} \equiv i\hat{\tau}_2$. Using this "complex" representation and the above mentioned passage from summation in $\mathbf{n}$ to integration in $\mathbf{r}$, we can write the pair contribution to γ in the form

$$\frac{c^2}{a^2} \mathrm{Im} \int_{r > r_0} \Re \frac{p(\mathbf{r}) + \hat{i} q(\mathbf{r})}{s(\mathbf{r}) + \hat{i} t(\mathbf{r})} d\mathbf{r}, \qquad (85)$$

with the functions $s(\mathbf{r}) = 1 - \tilde{V}^2\left[g_3^2(\mathbf{r}) - g_1^2(\mathbf{r})\right]$ and $t(\mathbf{r}) = -2\tilde{V}^2 g_3(\mathbf{r}) g_1(\mathbf{r})$ in the denominator and some functions $p(\mathbf{r}), q(\mathbf{r})$ in the numerator. Here the symbol $\Re$

means the "real" (traceful) part of the "complex" integrand, while the common imaginary part Im is produced by its poles. These are attained at such separations $\mathbf{r} = \mathbf{r}^*$ of impurity pairs that $s(\mathbf{r}^*) = t(\mathbf{r}^*) = 0$, which requires two conditions to be fulfilled:

$$|\, g_3(\mathbf{r}^*)\,| = \frac{1}{\tilde{V}}, \qquad g_1(\mathbf{r}^*) = 0. \tag{86}$$

Direct calculation in Eq. (80) at $\varepsilon = 0$ gives the amplitudes in Eq. (81) as

$$f_3(n_1, n_2) = \frac{\lambda_F \rho_N}{2} \frac{\beta n_1}{\beta^2 n_1^2 + n_2^2}, \tag{87}$$

with the Fermi wavelength $\lambda_F = 2\pi / k_F$, and also $f_1(n_1, n_2) = f_3(n_1, n_2)$. Using them in Eqs. (81), (86) shows that all possible $\mathbf{r}^*$ are isolated points on nodal directions, forming identical finite series along them (like those in Fig. 17). Also we note that poles only exist at high enough band filling, $\mu\rho_N \geq (1+\mathrm{e})^{-1}$ and strong enough perturbation parameter, $v \geq (1+g_{\mathrm{as}})^{-1}$, as chosen in Fig. 17. If so, it is suitable to pass in the vicinity of each $\mathbf{r}^*$ from integration in the components r_1, r_2 of the vector $\mathbf{r}$ to that in the components s, t of the "complex" denominator:

$$\mathrm{Im} \sum_{\mathbf{r}^*} \int ds dt \mathcal{J}_{\mathbf{r}^*}(s,t) \frac{p(s,t)s + q(s,t)t}{s^2 + t^2}, \tag{88}$$

where the transformation Jacobian

$$\mathcal{J}_{\mathbf{r}^*}(s,t) = \left. \frac{\partial(r_1, r_2)}{\partial(s,t)} \right|_{\mathbf{r}=\mathbf{r}^*}$$

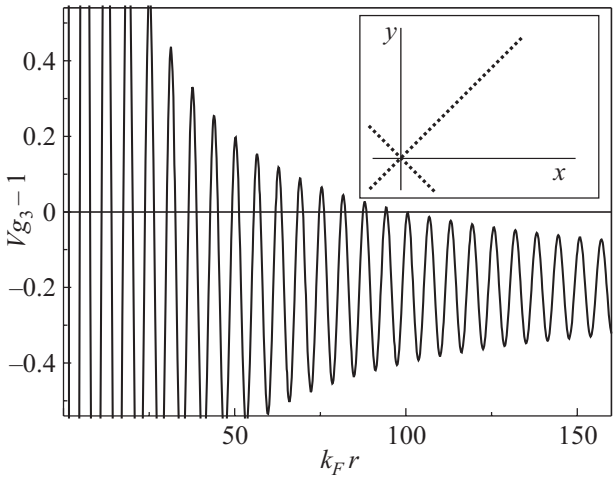

Fig. 17. Inset: the isolated poles of the integrand in Eq. (8) in function of pair separation vector $\mathbf{r} = (x, y)$, are located along the nodal axes in the direct space, where one of the pole conditions, $g_1(\mathbf{r}) = 0$, holds identically. Another pole condition, $|\, g_3(\mathbf{r})\,| = 1/|\,\tilde{V}\,| = |\, g_{\mathrm{as}} - 1/V\,|$, is reached at discrete points (here at the choice of parameters $\beta = 0.05$, $\tilde{V} g_{\mathrm{as}} = 5$). The main panel shows the related behavior of $\tilde{V} g_3(\mathbf{r}) - 1$ along the nodal direction of $\mathbf{r}$.

is real and nonsingular for any $\mathbf{r}^*$. Then a singularity in the denominator of Eq. (88) is canceled by a vanishing residue in the numerator and, even at formal existence of poles, they give *no contribution* to the zero energy DOS. Mathematically, this simply follows from an extra dimension at 2D integration, giving zero weights to isolated poles.

The above conclusion can be immediately generalized for any lth order GE term ($l \geq 3$), where the integrand is again presented as $(p + \hat{i}q)/(s + \hat{i}t)$ and p, q, s, t are now continuous functions of $N_l = 2(l-1)$ independent variables (components of the vectors $\mathbf{r}_1, \ldots, \mathbf{r}_{l-1}$) in the configurational space $\mathcal{S}_l$. This integrand can have simple poles on some $(N_l - 2)$-dimensional surface $\mathcal{A}_l$ in $\mathcal{S}_l$ (under easier conditions than for $l = 2$). Then the N_l-fold integration can be done over certain coordinates $u_1, \ldots, u_{N_l - 2}$ in $\mathcal{A}_l$ and over the components s, t of the "complex" denominator in the normal plane to $\mathcal{A}_l$:

$$\mathrm{Im} \int du_1 \ldots du_{N_l - 2} \mathcal{J}(u_1, \ldots, u_{N_l - 2}) \times$$

$$\times \int ds dt \frac{p(\ldots, s, t)s + q(\ldots, s, t)t}{s^2 + t^2}, \tag{89}$$

with a nonsingular Jacobian $\mathcal{J}$. The latter integral has no imaginary part by the same reasons as for Eq. (88). Thus, it can be concluded that perturbation by NM impurities in a *d*-wave system *can not* produce localized quasiparticles of zero energy, and this directly relates to the indicated isomorphism of the interaction matrices with the algebra $\mathbb{C}$ of complex numbers.

Moreover, the same conclusion is also valid for yet another type of NM-perturbation, due to locally perturbed SC order by the perturbation matrix $\hat{V} = V\hat{\tau}_1$. In this case, the interaction matrix:

$$\hat{A}_{\mathbf{n}} = \frac{V}{1 - V^2 g_{\mathrm{as}}^2} \{ g_1(\mathbf{n}) + V g_{\mathrm{as}} g_3(\mathbf{n}) +$$

$$+ i [\, g_3(\mathbf{n}) - V g_{\mathrm{as}} g_1(\mathbf{n})\,] \hat{\tau}_2 \},$$

pertains to the same family $\hat{C}(x, y)$ as in the above case, hence leading to the same absence of contribution to the zero energy DOS.

7.3. Magnetic impurities

However, an essential cluster contribution to zero energy DOS can be produced by M impurities with the scalar local perturbation $\hat{V} = \tilde{V}$ and the respective T-matrix (similar to Eq. (56)) in the zero energy limit:

$$\hat{T}(0) = \tilde{V}(1 - \tilde{V}\hat{G})^{-1} = \tilde{V} \frac{1 + v g_{\mathrm{as}} \hat{\tau}_3}{1 - v^2 g_{\mathrm{as}}^2}, \tag{90}$$

where $v = \tilde{V}\rho_N$. Unlike the traceless $\hat{T}(0)$ for NM impurities, this matrix produces a finite shift of the nodal point itself, from $\varepsilon = 0$ to $\varepsilon = \varepsilon_0 \approx c\tilde{V}/(1 - v^2 g_{\mathrm{as}}^2)$. As usually,

this shift can be absorbed into the Fermi level position by shifting all the energy arguments of considered GF's, then the DOS calculated in the T-matrix (or SCTMA) approximation will vanish at $\varepsilon \to \varepsilon_0$ (in the same way as it vanishes at $\varepsilon \to 0$ for NM impurities), fixing the distinguished point of quasiparticle spectrum in the case of M impurities. The following treatment of higher order GE terms involves the matrix of interaction between M impurities:

$$\hat{A}_{\mathbf{r}} = v\frac{(\hat{\tau}_3 + vg_{\text{as}})g_3(\mathbf{r}) + (\hat{\tau}_1 - ivg_{\text{as}}\hat{\tau}_2)g_1(\mathbf{r})}{1 - v^2 g_{\text{as}}^2}. \quad (91)$$

Notably, this matrix does not fit the $\mathbb{C}$-algebra, and, though being harder technically, this allows effective contribution by M impurities to the zero energy DOS. In fact, the straightforward calculation of the corresponding GE pair term leads to the general matrix expression:

$$(1 - \hat{A}_{\mathbf{r}}\hat{A}_{-\mathbf{r}})^{-1} = \frac{N_0 - N_1\hat{\tau}_1 - iN_2\hat{\tau}_2 - N_3\hat{\tau}_3}{D_{\mathbf{r}}}. \quad (92)$$

Here N_j's and $D_{\mathbf{r}}$ are the following functions of $g_1(\mathbf{r})$ and $g_3(\mathbf{r})$:

$$N_0 = (2+\delta)v^2 g_1^2 + \delta v^2 g_3^2 + \delta^2,$$

$$N_1 = 2v^2\sqrt{1+\delta}\,g_1 g_3, \quad N_2 = 2v^2(1+\delta)g_1 g_3,$$

$$N_3 = 2v^2\sqrt{1+\delta}\,g_3^2,$$

$$D_{\mathbf{r}} = (8+6\delta)v^4 g_1^2 g_3^2 + \left[4v^2 g_1^2 + v^4(g_1^4 + g_3^4)\right]\delta +$$

$$+ 2v^2(g_1^2 + g_3^2)\delta^2 + \delta^3, \quad (93)$$

with the parameter $\delta = 1 - v^2 g_{\text{as}}^2$. Zeroes of D in the space of variables g_1, g_3 form certain continuous trajectories shown in Fig. 18 (cf. to their location in the isolated points $g_1(\mathbf{r}) = 0, \pm g_3(\mathbf{r}) = g_{\text{as}} + 1/v$, in the NM case). It is just this extension of singularities, from isolated points to continuous trajectories, that allows the imaginary part of the 2D integral

$$\sigma \approx c^2\tilde{V}\delta\,\text{Im}\int \frac{d\mathbf{r}}{a^2}\frac{N_0 - \sqrt{1+\delta}N_3}{D_{\mathbf{r}}} \quad (94)$$

to be finite. On the other hand, this is assured by the fact that the traceful numerator in Eq. (94) does not vanish on these trajectories. Quantitative analysis is simplified in the case of $|\delta| \ll 1$ defines a low-energy resonance at $\varepsilon_{\text{res}} \approx \Delta\delta/[v\ln(1/\delta^2)]$ [85]. In this case the numerator in Eq. (94) is simplified as $N_0 - \sqrt{1+\delta}N_3 \approx 2v^2(g_1^2 - g_3^2)$. Using the functions $g_1(\mathbf{r}), g_3(\mathbf{r})$ from Eqs. (81), (87), it can be shown that the pole trajectories, $D_{\mathbf{r}} = 0$, when presented in variables $r_{1,2}$, form multiple loops (seen in Fig. 19,*a*) of total number $\sim 1/(\beta|\delta|)$, each contributing by $\sim \pi^2/[(ak_F)^2|\delta|]$ into $(Va)^{-2}\,\text{Im}\int d\mathbf{r} g_{\mathbf{r}}^2/D_{\mathbf{r}}$ in

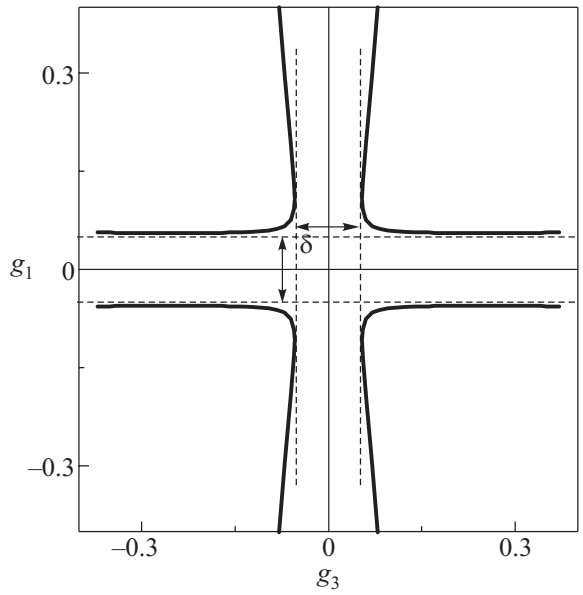

Fig. 18. Trajectories in the space of variables $g_1(\mathbf{r}), g_3(\mathbf{r})$, corresponding to the poles of GE denominator, Eq. (93), for M impurities at the choice of $v = 1$ and $\delta = 0.1$.

Eq. (86). Thus we arrive at the estimate: $\sigma \sim c^2\tilde{V}/|\delta|$, and hence to the finite residual DOS:

$$\rho(\varepsilon_0) \sim \rho_N \frac{c^2\tilde{V}}{\Delta|\delta|}\ln\frac{\Delta|\delta|}{c^2\tilde{V}}. \quad (95)$$

We recall that this result is impossible in the properly formulated self-consistent approximation [55], and it is also in a striking difference to the SCTMA predictions, $\rho(0) \sim \exp(-\rho_N\Delta/cv^2)\rho_N^2\Delta/(cv^2)$ in the Born limit [75] or $\rho(0) \sim \sqrt{c\rho_N/\Delta}$ in the unitary limit [36]. The nonuniversality of this effect is manifested by its sensitivity to the M-perturbation parameter v, so that $\rho(\varepsilon_0)$ is mostly defined by impurity pairs only for strong enough perturbations, $|v| \gtrsim (1+g_{\text{as}})^{-1}$. For weaker v, nodal quasiparticles will be only localized on impurity clusters of a greater number $n > 2$ (the bigger the smaller $|v|$), and the particular form of Eq. (87) would change to $\rho(0) \sim \rho_N c^n$ (with some logarithmic corrections). Anyhow, a finite limit of DOS at zero energy is granted by the fact that in real high-T_c systems a certain M-type perturbation can result even from nominally nonmagnetic centers (as shown in Sec. 5.2). Moreover, the above considered condition $|v|g_{\text{as}} \approx 1$ does not seem very difficult, as testified by the observation of extremely low-energy resonance $\varepsilon_{\text{res}} \approx -1.5$ meV by Zn impurities in $Bi_2Sr_2CaCu_2O_{8+\delta}$ [18]. It just fits the asymmetric M resonance from Fig. 20, contrasting with the symmetric NM resonance picture.

Then the overall impurity effect in a *d*-wave superconductor can be seen as a superposition (almost independent) of the above described effects from NM

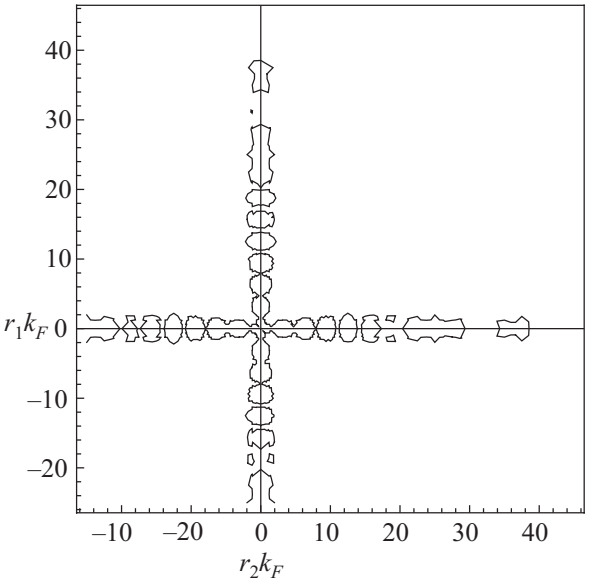

Fig. 19. In the **r**-plane, the trajectories of zeroes of $D_{\mathbf{r}}$ form continuous loops within the stripes of $\sim v_F/(v_\Delta|\delta|k_F)$ length and $\sim 1/(|\delta|k_F)$ width along the nodal axes.

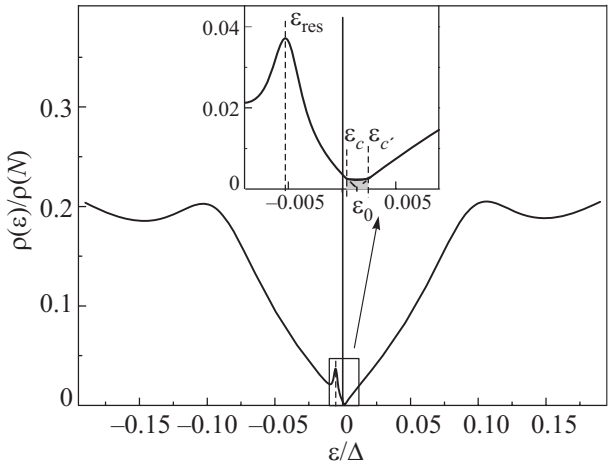

Fig. 20. Low-energy *d*-wave DOS $\rho(\varepsilon)$ in simultaneous presence of NM impurities (with $c_{NM} = 3\%$ and $v_{NM} = 1$), producing two symmetric broad resonances, and M impurities (with $c = 0.03\%$, $v = v_{NM}$, and $vg_{as} = 0.9$), producing single sharp resonance at extremely low energy ε_{res}. Inset shows the mobility edges ε_c and $\varepsilon_{c'}$ around the shifted nodal point ε_0, they separate localized states (shadowed area) with almost constant DOS, $\rho(\varepsilon) \approx \rho(\varepsilon_0)$, from band-like states whose DOS is close to the T-matrix value (solid line).

impurities with perturbation parameter V_{NM} and concentration c_{NM} and from M impurities with perturbation parameter V and concentration c (supposedly $c \ll c_{NM}$). An example of such situation is shown in Fig. 20.

The residual DOS from pair GE term prevails within a certain narrow vicinity of ε_0 where quasiparticle states are all localized on properly separated impurity pairs. Outside this vicinity, the states are extended and reasonably described by T-matrix (or SCTMA). The transition from localized to extended states occurs at the Mott mobility edges $\varepsilon_c < \varepsilon_0$ and $\varepsilon_{c'} > \varepsilon_0$, where GE and T-matrix contributions to DOS are comparable. Using the simplest approximation for the T-matrix term: $\rho(\varepsilon) \sim \rho_N |\varepsilon - \varepsilon_0|/\Delta$, we estimate the range of localized states (somewhat exaggerated in the inset of Fig. 20) as

$$\varepsilon_{c'} - \varepsilon_0 \sim \varepsilon_0 - \varepsilon_c \sim \delta_c \sim \frac{c^2\tilde{V}}{|\delta|}\ln\frac{\Delta|\delta|}{c^2\tilde{V}}, \qquad (96)$$

provided it is much smaller than the distance to the M resonance: $\delta_c \ll |\varepsilon_0 - \varepsilon_{res}|$. The same estimates for the mobility edges follow from the IRM breakdown condition: $\varepsilon - \mathrm{Re}\,\Sigma(\varepsilon) \sim \mathrm{Im}\,\Sigma(\varepsilon)$, at $\varepsilon \approx \varepsilon_0$.

The tendency to localization of quasiparticles can be generally opposed by the effects of repulsive Coulomb interaction between them [21] and this issue was also discussed for disordered *d*-wave superconductors [87,88]. These field theory treatments showed that localization can survive at low enough temperature. The full account of Coulomb interactions in the present GE approach is rather complicated technically, but a simple estimate follows from the overall number of (supposedly) localized particles within the energy range, Eq. (96), which is as small as $n_{loc} \sim \rho(\varepsilon_0)\delta_c \sim (c^4\tilde{V}/\Delta\delta^2)\ln^2|\Delta\delta/c^2\tilde{V}|$. Since the average distance between them $\sim a/\sqrt{n_{loc}}$ is much longer than the distance between charge carriers $\sim a/\sqrt{n} \sim a/\sqrt{\rho_N\varepsilon_F}$, the effects of Coulomb interaction are hopefully screened out, at least for the systems far enough from half-filling [89]. Notably, localization turns to be yet possible near the resonance energy, $\varepsilon \approx \varepsilon_{res}$, but this requires that the concentration of M impurities surpasses a certain characteristic value $c_{res} \sim (\varepsilon_{res}/\Delta)^2 \ln(\Delta/|\varepsilon_{res}|)$. In particular, for the choice of parameters in Fig. 20, we find $c_{res} \sim 3\cdot 10^{-4}$, so that this system should be close to the onset of localization also in this spectrum range, where each localized state is associated with a *single* impurity center.

Generally, presence of localized states near the lowest excitation energies in the spectrum must influence significantly the kinetic properties of a crystal with impurities, such as electric and (electronic part of) heat conductivity at lowest temperatures. Taking in mind the above referred modification of Kubo formula for the energy range $|\varepsilon - \varepsilon_0| < \delta_c$, their temperature dependencies, instead of reaching the universal values σ_0 and $[\kappa/T](0)$, should rather tend to the exponential vanishing: $\sim \exp(-\delta_c/k_BT)$, at low enough temperatures: $T \ll \delta_c/k_B$. The latter value, at the same choice of impurity perturbation parameters and typical gap $\Delta \sim 30$ meV, is estimated as ~ 0.2 K. In this context, the intriguing sharp downturn of κ/T, recently observed at temperatures $\lesssim 0.3$ K [41] and attributed to the

low-temperature decoupling of phonon heat channel [42], can be otherwise considered as a possible experimental manifestation of the quasiparticle localization by impurity clusters. A more detailed analysis of possible nonuniversal behavior of transport properties of disordered *d*-wave superconductors will be necessary to confirm this conjecture.

8. Interaction between impurities and collapse of antinodal quasiparticles

Now we pass to the physics near the antinodal points, corresponding to another special energy in quasiparticle spectrum of pure *d*-wave superconductor, characterized by the logarithmic singularity of DOS, Eq. (13). In presence of impurities, this singularity is broadened and the issue of quasiparticle localization is in order. The anomalous behavior of electronic excitations near the antinodal points was recently recognized in ARPES data [90–92] on *d*-wave high-T_c superconductors and a description of the peculiar spectral density function characterized by a new energy scale was proposed within the dynamical mean-field method [93]. Here we develop an alternative approach to this problem, along the same lines as in Sec. 7 for low energies, beginning from the simple T-matrix, Eq. (32), or SCTMA, Eq. (65), and using the IRM criterion, Eq. (73). Since the relevant GF $g_0(\varepsilon-\Sigma_0)$ at $\varepsilon \approx \Delta$ is dominated by the big imaginary part, its relation to the self-energy can be written in a "unitary limit" form:

$$g_0(\varepsilon-\Sigma_0) \approx \frac{c}{\rho_N \Sigma_0(\varepsilon)}$$

(for definiteness, nonmagnetic impurities are considered). Using here the logarithmic approximation, $g_0(\varepsilon) \approx \ln(4\Delta/\sqrt{\Delta^2-\varepsilon^2})$, we arrive at the estimate:

$$\Sigma_0(\Delta) \approx \frac{ic}{\rho_N \ln\left(4\rho_N \Delta / c\right)}.$$

Then the IRM criterion: $\Delta \gg \mathrm{Im}\Sigma_0(\Delta)$, is fulfilled for the SCTMA solution if the impurity concentration c is well below the characteristic "antinodal" value:

$$c_{AN} \approx \rho_N \Delta \ln\left(\frac{1}{\rho_N \Delta}\right). \qquad (97)$$

This would mean that for $c < c_{AN}$ band quasiparticles survive in the whole of antinodal areas. However, by the same reason as in Sec. 7, this conclusion needs yet to be checked with respect to the effects of interaction between impurities, displayed by the GE terms. The specifics of the antinodal area is the hyperbolic structure of isoenergetic lines, $\varepsilon^2-\Delta^2 = \xi^2-\eta^2$, instead of the elliptic structure, Eq. (82), in the nodal area. Here the variables $\xi = \hbar v_F q_1$ and $\eta = \hbar v_\Delta q_2$ are formally the same as in the nodal case, but related to the 1- and 2-components along the Cartesian

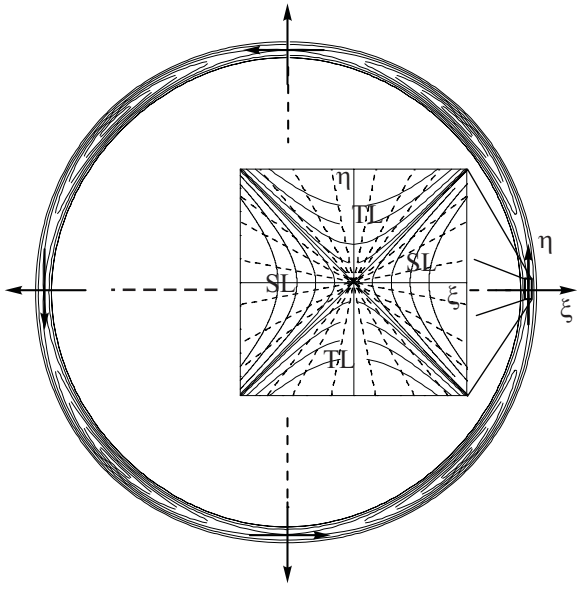

Fig. 21. Isoenergetic lines for *d*-wave dispersion law display elliptic structure near nodal points and hyperbolic structure near antinodal points. Inset shows how these lines near an antinodal point give rise to the hyperbolic coordinates E (solid lines) and t (dashed lines) in the "spacelike" (SL) and "timelike" (TL) sectors of the ξ, η plane.

x, y axes (Fig. 21), instead of the diagonals in the nodal case. Then the amplitudes in Eq. (79) for the matrices $\hat{A}_{\mathbf{n}}$ can be estimated with the same infinite extension of integration limits:

$$f_0(x,y) \approx \frac{\rho_N}{4} \int_{-\infty}^{\infty} d\eta \int_{-\infty}^{\infty} d\xi \frac{e^{i(\beta x \xi + y\eta)k_F/\Delta}}{\tilde{\varepsilon}^2 - \xi^2 + \eta^2}, \qquad (98)$$

where the small energy parameter $\tilde{\varepsilon}^2 \equiv \varepsilon^2 - \Delta^2$ defines the longest decay lengths (see below).

This integration is most naturally done in the hyperbolic variables E and t for energy, defined in a proper way for different sectors of the ξ, η plane, "spacelike" (SL) with $\xi^2 > \eta^2$ and "timelike" (TL) with $\xi^2 < \eta^2$:

$$\begin{cases} \xi = E\cosh t, & \eta = E\sinh t \quad \text{(SL)}, \\ \xi = E\sinh t, & \eta = E\cosh t \quad \text{(TL)}. \end{cases}$$

Similar hyperbolic variables for position, r and τ, are defined in the "spacelike" (sl), $\beta^2 x^2 > y^2$, and "timelike" (tl), $\beta^2 x^2 < y^2$, sectors of x, y plane:

$$\begin{cases} \beta x = r\cosh\tau, & y = r\sinh\tau \quad \text{(sl)}, \\ \beta x = r\sinh\tau, & y = r\cosh\tau \quad \text{(tl)}. \end{cases}$$

Then, for positions from the sl-sectors (but not too close to their borders), the amplitude in Eq. (98) is represented as

$$f_0(x,y) \approx \rho_N \left\{ \int_0^\infty E\,dE \int_0^\infty dt \left[\frac{\cos\left(\frac{Ek_F r}{\Delta} \cosh t \right)}{\tilde{\varepsilon}^2 - E^2} + \right.\right.$$

$$\left.\left. + \frac{\cos\left(\frac{Ek_F r}{\Delta} \sinh t \right)}{\tilde{\varepsilon}^2 + E^2} \right] \right\}, \qquad (99)$$

and these integrals are done analytically:

$$f_0(x,y) \approx \frac{\pi\rho_N}{4} \left[G^{3,1}_{1,1}\left(\begin{matrix} 0,-1/2 \\ 0,0,0;-1/2 \end{matrix} \middle| -\frac{\tilde{\varepsilon}^2 k_F^2 r^2}{4\Delta^2} \right) + \right.$$

$$\left. + G^{3,-}_{-,1}\left(\begin{matrix} 0,- \\ 0,0,0;- \end{matrix} \middle| -\frac{\tilde{\varepsilon}^2 k_F^2 r^2}{4\Delta^2} \right) \right]. \qquad (100)$$

Here the first from the Meijer G-functions, $G^{3,1}_{1,1}$ [49], is almost coincident with the Hankel function by Eq. (83), but for $\varepsilon \approx \Delta$ and the argument written as $\sqrt{x^2/\tilde{\ell}_F^2 - y^2/\tilde{\ell}_\Delta^2}$ with the decay lengths $\tilde{\ell}_i = \hbar v_i / \tilde{\varepsilon}$, while the second G-function, $G^{3,-}_{-,1}$, is much faster decaying. Similar expressions for the tl-sectors involve the argument $\sqrt{y^2/\tilde{\ell}_\Delta^2 - x^2/\tilde{\ell}_F^2}$.

However the validity of the above approximation is limited in distances x, y. Thus, alike the low-energy case of Sec. 7, the formal divergence of the function, Eq. (100), at approaching the sector borders, $\beta^2 x^2 \to y^2$, is restricted to a finite value $\sim \rho_N \cos(\tilde{\varepsilon} k_F y / \Delta)$, corresponding to distances $|\beta x - y| \sim a\Delta / \tilde{\varepsilon}$. Also, due to the actually finite integration range in E, t, the decay length for f_0 along these borders is limited to $\sim a\mu / \Delta$. The general characteristics of the resulting interaction is its contribution to the GE pair term from the set of contours in the x, y plane within the stripes of $\sim a\Delta / \tilde{\varepsilon}$ width and $\sim a\mu / \Delta$ length along the $\beta^2 x^2 = y^2$ lines. This contribution is estimated as

$$cB \sim \frac{c\mu}{|\tilde{\varepsilon}| \ln(\mu / |\tilde{\varepsilon}|)}, \qquad (101)$$

and its comparison with unity defines the GE convergence range outside the energy range of

$$|\tilde{\varepsilon}| \sim \Delta \frac{c\mu}{\Delta \ln(\mu/\Delta)} \sim \Delta \frac{c}{c_{AN}}. \qquad (102)$$

Thus we can expect that in the presence of the considered impurities in a d-wave superconductor, even at their low concentration $c \ll c_{AN}$, there is a narrow vicinity of antinodal line at the Fermi surface, defined by Eq. (102), where GE, Eq. (28), becomes to diverge and so the band quasiparticles can not exist (Fig. 22). Within this vicinity, the excited quasiparticles are localized on various clusters of close impurities. This also defines a new energy scale in the quasiparticle spectrum, related to the impurity concentration by Eq. (102).

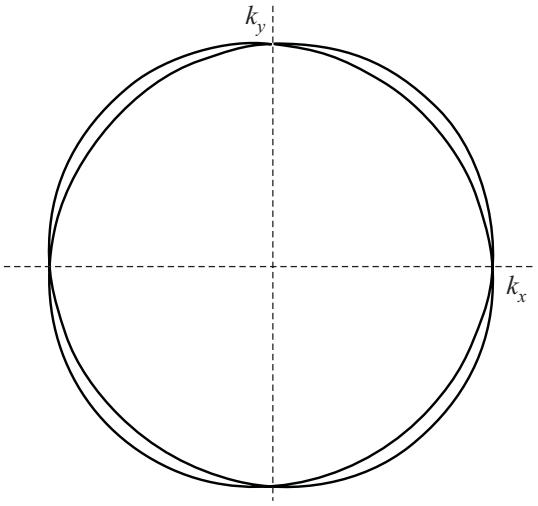

Fig. 22. Narrow areas (seen as solid lines) in the Brillouin zone of a d-wave superconductor with low concentration of impurities, $c \ll c_{AN}$, where the quasiparticle states are no more described by the band dispersion law but localized on clusters of close impurities.

A similar destroying of band dispersion of quasiparticles near the van Hove singularities in the spectrum of a d-wave superconductor can also result from quasiparticle scattering by other mechanisms (electron–electron, electron–phonon, etc.).

9. Conclusions

The quasiparticle states are considered in a d-wave superconductor with impurities, extending the self-consistent T-matrix approximation framework by using the techniques of group expansions of Green functions in complexes of interacting impurities. A comparative analysis of impurity effects on quasiparticle energy and lifetime is done for different types of impurity perturbations, varying their intensity, spatial extent, and matrix structure in Nambu indices. The essential difference between point-like and extended perturbation is established, consisting in separate action of different symmetry modes of perturbation on different physical properties of quasiparticles, which eventually reduces destructive effects of extended impurity centers on SC order. Using the Ioffe–Regel–Mott criterion, modified for the case of quasiparticles in d-wave superconductors, the criteria of validity are established for SCTMA and a proper combination of different self-consistent solutions for different regions of energy spectrum is suggested. Beyond the scope of SCTMA, the practical calculation of group expansions for different types of impurities is developed. It

is shown that, if the impurity perturbation of magnetic type is present, the indirect interaction between impurities can essentially change the quasiparticle spectrum near nodal points, producing strongly localized states of nonuniversal character (depending on the perturbation strength). Experimental check for possible nonuniversal effects in low-temperature transport properties can be done, e.g., in the Zn doped $Bi_2Sr_2CaCu_2O_{8+\delta}$ system.

1. J.G. Bednorz and K.A. Müller, *Z. Phys.* **B64**, 189 (1986).
2. M.K. Wu, J.R. Ashburn, C.J. Torng, P.H. Hor, R.L. Meng, L. Gao, Z.J. Huang, Y.Q. Wang, and C.W. Chu, *Phys. Rev. Lett*. **58**, 908 (1987).
3. D.M. Ginsberg (ed.), *Physical Properties of High-Temperature Superconductors V*, World Scientific, Singapore (1996).
4. A.V. Balatsky, I. Vekhter, and J.X. Zhu, *Rev. Mod. Phys*. **78**, 373 (2006).
5. P.W. Anderson, *J. Phys. Chem. Solids* **11**, 26 (1959).
6. P.G. de Gennes, *Superconductivity of Metals and Alloys*, Perseus Books Publishing, L.L.C. (1999).
7. A.A. Abrikosov and L.P. Gor'kov, *Sov. Phys. JETP* **12**, 1243 (1961).
8. M. Fowler and K. Maki, *Phys. Rev*. **164**, 484 (1967).
9. H. Shiba, *Prog. Theor. Phys*. **40**, 435 (1968).
10. A.I. Rusinov, *JETP Lett. URSS* **9**, 85 (1969).
11. W.E. Pickett, *Rev. Mod. Phys*. **61**, 433 (1989).
12. C.C. Tsuei and J.R. Kirtley, *Rev. Mod. Phys*. **72**, 969 (2000).
13. D.A. Bonn, S. Kamal, K. Zhang, R. Liang, D.J. Baar, E. Klein, and W.N. Hardy, *Phys. Rev.* **B50**, 4051 (1994).
14. A.V. Balatsky, M.I. Salkola, and A. Rozengren, *Phys. Rev.* **B51**, 15547 (1995).
15. Yu.G. Pogorelov, *Solid State Commun*. **95**, 245 (1995).
16. J.M. Valles, Jr., R.C. Dynes, A.M. Cucolo, M. Gurvitch, L.F. Schneemeyer, J.P. Garno, and J.V. Waszczak, *Phys. Rev.* **B44**, 11986 (1991).
17. A. Yazdani, C.M. Howald, C.P. Lutz, A. Kapitulnik, and D.M. Eigler, *Phys. Rev. Lett*. **83**, 176 (1999).
18. S.H. Pan, E.W. Hudson, K.M. Lang, H. Eisaki, S. Ushida, and J.C. Davis, *Nature (London)* **403**, 746 (2000).
19. E.W. Hudson, K.M. Lang, V. Madhavan, S.H. Pan, H. Eisaki, S. Ushida, and J.C. Davis, *Nature (London)* **411**, 920 (2001).
20. W.N. Hardy, S. Kamal, D.A. Bonn, K. Zhang, R. Liang, D.C. Morgan, and D.J. Baar, *Physica* **B197**, 609 (1994).
21. D.N. Basov, A.V. Puchkov, R.A. Hughes, T. Strach, J. Preston, T. Timusk, D.A. Bonn, R. Liang, and W.N. Hardy, *Phys. Rev.* **B49**, 12165 (1991).
22. S.G. Doettinger, R.P. Huebener, P. Gerdermann, A. Kühle, S. Anders, T.G. Träuble, and J.C. Villégier, *Phys. Rev. Lett*. **73**, 1691 (1994).
23. F. Guinea and Yu. Pogorelov, *Phys. Rev. Lett*. **74**, 462 (1995).
24. L. Taillefer, B. Lussier, R. Gagnon, K. Behnia, and H. Aubin, *Phys. Rev. Lett*. **79**, 483 (1997).
25. M. Sutherland, D.G. Hawthorn, R.W. Hill, F. Ronning, S. Wakimoto, H. Zhang, C. Proust, E. Boaknin, C. Lupien, L. Taillefer, R. Liang, D.A. Bonn, W.N. Hardy, R. Gagnon, N.E. Hussey, T. Kimura, M. Nohara, and H. Takagi, *Phys. Rev.* **B67**, 174520 (2003).
26. I.M. Lifshitz, *Adv. Phys*. **13**, 483 (1964).
27. N.F. Mott, *Adv. Phys*. **16**, 49 (1967).
28. P.W. Anderson, *Phys. Rev*. **109**, 1492 (1958).
29. T. Matsubara, *Prog. Theor. Phys*. **14**, 351 (1955).
30. D.N. Zubarev, *Sov. Phys. Uspekhi* **3**, 320 (1960).
31. A.A. Abrikosov, L.P. Gor'kov, and I.E. Dzyaloshinskii, *Methods of Quantum Field Theory in Statistical Physics,* Dover Publications, NY (1975).
32. L.P. Gor'kov, *Sov. Phys. JETP* **7**, 505 (1958).
33. C.J. Pethick and D. Pines, *Phys. Rev. Lett*. **57**, 118 (1986).
34. S. Schmitt-Rink, K. Miyake, and C.M. Varma, *Phys. Rev. Lett*. **57**, 2575 (1986).
35. P.J. Hirshfeld, P. Wolfle, and D. Einzel, *Phys. Rev.* **B37**, 83 (1988).
36. P.A. Lee, *Phys. Rev. Lett*. **71**, 1887 (1993).
37. M.J. Graf, S.-K. Yip, J.A. Sauls, and D. Rainer, *Phys. Rev.* **B53**, 15147 (1996).
38. A.C. Durst and P.A. Lee, *Phys. Rev.* **B62**, 12070 (2000).
39. K.S. Novoselov, A.K. Geim, S.V. Morozov, D. Jiang, Y. Zhang, S.V. Dubonos, I.V. Grigorieva, and A.A. Firsov, *Science* **306**, 666 (2004).
40. N.M.R. Peres, F. Guinea, and A.H. Castro Neto, *Phys. Rev.* **B73**, 125411 (2006).
41. R.W. Hill, C. Proust, L. Taillefer, R. Fournier, and R.L. Greene, *Nature* **414**, 711 (2001).
42. M.F. Smith, J. Paglione, M.B. Walker, and L. Taillefer, *Phys. Rev*. **B71**, 014506 (2005).
43. M.A. Ivanov, *Sov. Phys. Solid State* **12**, 1508 (1971).
44. J.E. Mayer and M. Goeppert-Mayer, *Statistical Mechanics,* Wiley, NY (1940).
45. M.A. Ivanov, V.M. Loktev, and Yu.G. Pogorelov, *Phys. Rep*. **153**, 209 (1987).
46. F.C. Zhang and T.M. Rice, *Phys. Rev.* **B37**, 3759 (1988).
47. A. Fujimori, *Phys. Rev.* **B39**, 793 (1989).
48. V.A. Gavrichkov, E.V. Kuz'min, and S.G. Ovchinnikov, *Phys. Uspekhi* **43**, 1813 (2000).
49. M. Abramowitz and I.A. Stegun, *Handbook of Mathematical Functions,* National Bureau of Standards, NY (1964).
50. M. Franz, C. Kallin, and A.J. Berlinsky, *Phys. Rev.* **B54**, R6897 (1996).
51. W.A. Atkinson, P.J. Hirschfeld, and A.H. McDonald, *Phys. Rev. Lett*. **85**, 3922 (2000).
52. A. Polkovnikov, S. Sachdev, and M. Voyta, *Phys. Rev. Lett*. **86**, 296 (2001).
53. G. Baym, *Phys. Rev*. **127**, 1391 (1962).
54. M.A. Ivanov and Yu.G. Pogorelov, *Sov. Phys. JETP* **72**, 2198 (1977).
55. V.M. Loktev and Yu.G. Pogorelov, *Fiz. Nizk. Temp*. **27,** 1039 (2001) [*Low Temp. Phys*. **27**, 767 (2001)].
56. L. Zhu, W.A. Atkinson, and P.J. Hirschfeld, *Phys. Rev.* **B69**, 060503(R) (2004).

57. I. Adagideli, P.M. Golgbart, A. Schnirman, and A. Yazdani, *Phys. Rev. Lett*. **83**, 5571 (2001).
58. Yu.G. Pogorelov and M.C. Santos, *Phys. Rev.* **B71**, 014516 (2005).
59. F.A. Cotton, *Chemical Applications of Group Theory,* Wiley, NY (1990).
60. Yu.A. Izyumov and M.V. Medvedev, *Magnetically Ordered Crystals Containing Impurities,* Consultants Bureau, NY (1973).
61. T.R. Chien, Z.Z. Chang, and N.P. Ong, *Phys. Rev. Lett*. **67**, 2088 (1991).
62. P.J. Hirschfeld and N. Golgenfeld, *Phys. Rev.* **B48**, 4219 (1993).
63. R. Fehrenbacher and M.R. Norman, *Phys. Rev.* **B50**, 3495 (1994).
64. A.V. Mahajan, H. Alloul, G. Collin, and J.F. Marucco, *Phys. Rev. Lett*. **72**, 3100 (1994).
65. W.A. MacFarlane, J. Bobroff, H. Alloul, P. Mendels, and N. Blanchard, *Phys. Rev. Lett*. **85**, 11080 (2000).
66. Q. Chen and R.J. Schrieffer, *Phys. Rev.* **B66**, 014512 (2002).
67. K. Park, *Phys. Rev.* **B67**, 094513 (2003).
68. V.M. Loktev and Yu.G. Pogorelov, *Europhys. Lett*. **60**, 757 (2002).
69. R.E. Walstedt, R.F. Bell, L.F. Schneemeyer, and J.V. Waszczak, *Phys. Rev.* **B48**, 10646 (1993).
70. M.-H. Julien, T. Fehér, M. Horvatić, C. Berthier, O.N. Bakharev, P. Ségransan, G. Collin, and J.-F. Marucco, *Phys. Rev. Lett*. **84**, 3422 (2000).
71. R.J. Birgeneau and G. Shirane, in: *Physical Properties of High Temperature Superconductors I*, D.M. Ginsberg (ed.), World Scientific, Singapore (1989).
72. J. Kondo, *Progr. Theor. Phys*. **32**, 37 (1964).
73. Y. Nagaoka, *Phys. Rev*. **138**, A1112 (1965).
74. J. Zittartz and E. Mueller-Hartmann, *Z. Phys*. **232**, 11 (1970).
75. L.P. Gor'kov and P.A. Kalugin, *Sov. Phys. JETP Lett*. **41**, 253 (1985).
76. T. Senthil, M.P.A. Fisher, L. Balents, and C. Nayak, *Phys. Rev. Lett*. **81**, 4704 (1998).
77. A.A. Nersesyan, A.M. Tsvelik, and F. Wenger, *Nucl. Phys.* **B438**, 561 (1995).
78. K. Ziegler, M.H. Hetter, and P.J. Hirschfeld, *Phys. Rev. Lett*. **77**, 3013 (1996).
79. C. Pepin and P.A. Lee, *Phys. Rev. Lett*. **81**, 2779 (1998).
80. R.J. Elliott, J.A. Krumhansl, and P.L. Leath, *Rev. Mod. Phys*. **46**, 465 (1974).
81. V.M Loktev and Yu.G. Pogorelov, *Europhys. Lett*. **58**, 549 (2002).
82. A.F. Ioffe and A.R. Regel, *Progr. Semicond*. **4**, 237 (1960).
83. V.M. Loktev and Yu.G. Pogorelov, *Phys. Lett.* **A320**, 307 (2004).
84. L. Zhu, W.A. Atkinson, and P.J. Hirschfeld, *Phys. Rev*. **B67**, 094508 (2003).
85. Yu.G. Pogorelov and V.M. Loktev, *Phys. Rev.* **B69**, 214508 (2004).
86. Yu.G. Pogorelov, M.C. Santos, and V.M. Loktev, *cond-mat*/0605424 (2006).
87. D.V. Khveschenko, A.G. Yashenkin, and I.V. Gornyj, *Phys. Rev. Lett.* **86**, 4668 (2001).
88. M. Fabrizio, L. Del'Anna, and C. Castellani, *Phys. Rev. Lett*. **88**, 076603 (2002).
89. L. Boeri, E. Cappelluti, C. Grimaldi, and L. Pietronero, *Phys. Rev*. **B68**, 214514 (2003).
90. A. Kaminski, M. Randeria, J.C. Campuzano, M.R. Norman, H. Fretwell, J. Mesot, T. Sato, T. Takahashi, and K. Kadowaki, *Phys. Rev. Lett*. **86**, 1070 (2001).
91. T. Sato, H. Matsui, T. Takahashi, H. Ding, H.-B. Yang, S.-C. Wang, T. Fujii, T. Watanabe, A. Matsuda, T. Terashima, and K. Kadowaki, *Phys. Rev. Lett*. **91**, 157003 (2003).
92. M. Le Tacon, A. Sacuto, A. Georges, G. Kotliar, Y. Gallais, D. Colson, and A. Forget, *Nature Physics* **2**, 537 (2006).
93. M. Civelli, B.G. Kotliar, T.D. Stanescu, M. Capone, A. Georges, K. Haule, and O. Parcollet, *arXiv: 0704.1486v1* (2007).